# Magnetic interactions and possible structural distortion in kagome FeGe from first-principles study and symmetry analysis

Hanjing Zhou, <sup>1, 2, \*</sup> Songsong Yan, <sup>1, 2, \*</sup> Dongze Fan, <sup>1, 2</sup> Di Wang, <sup>1, 2, †</sup> and Xiangang Wan<sup>1, 2</sup>

<sup>1</sup>National Laboratory of Solid State Microstructures and School of Physics, Nanjing University, Nanjing 210093, China <sup>2</sup>Collaborative Innovation Center of Advanced Microstructures, Nanjing University, Nanjing 210093, China (Dated: November 29, 2022)

Recently, charge density wave (CDW) order has been discovered in a magnetic kagome metal FeGe, providing a new platform to explore the possible connection between magnetism and CDW in a kagome lattice. Based on density functional theory and symmetry analysis, we present a comprehensive investigation of electronic structure, magnetic properties and possible structural distortion of FeGe. We estimate the magnetic parameters including Heisenberg and Dzyaloshinskii-Moriya (DM) interactions, and find that the ferromagnetic nearest-neighbor  $J_1$  dominates over the others, while the magnetic interactions between nearest kagome layers favors antiferromagnetic. The Néel temperature  $T_N$  and Curie-Weiss temperature  $\theta_{CW}$  are successfully reproduced, and the calculated magnetic anisotropy energy is also in consistent with the experiment. However, these reasonable Heisenberg interactions and magnetic anisotropy cannot explain the double cone magnetic transition, and the DM interactions, which even exist in the centrosymmetric materials, can result in this small magnetic cone angle. Unfortunately, due to the crystal symmetry of the high-temperature structure, the net contribution of DM interactions to double cone magnetic structure is absent. Based on the experimental  $2 \times 2 \times 2$  supercell, we thus explore the subgroups of the parent phase. Group theoretical analysis reveals that there are 68 different distortions, and only four of them (space group P622 or  $P6_322$ ) without inversion and mirror symmetry thus can explain the lowtemperature magnetic structure. Furthermore, we suggest that these four proposed CDW phases can be identified by using Raman spectroscopy. Since DM interactions are very sensitive to small atomic displacements and symmetry restrictions, we believe that symmetry analysis is an effective method to reveal the interplay of delicate structural distortions and complex magnetic configurations.

### I. INTRODUCTION

Kagome lattices are emerging as an exciting platform for the rich emergent physics, including magnetism, charge density wave (CDW), topology, and superconductivity [1–43]. Three key features have been identified in the electronic structure associated with its lattice geometry, which are flat band derived from the destructive phase interference of nearest-neighbour hopping, topological Dirac crossing at K point in the Brillouin zone (BZ), and a pair of van Hove singularities (vHSs) at M point [2–5]. When large density of states from the kagome flat bands are located near the Fermi level, strong electron correlations can induce magnetic order [2, 3]. There are several magnetic kagome materials, such as FeSn [6-10],  $Fe_3Sn_2$  [11-14],  $Mn_3Sn$  [15],  $Co_3Sn_2S_2$  [16] and  $AMn_6Sn_6$  (A=Tb, Y) [17, 18], which usually exhibit magnetic order with ferromagnetically ordered layers that are either ferromagnetically or antiferromagnetically stacked. Meanwhile, when vHSs are located near the Fermi level, interaction between the saddle points and lattice instability could induce symmetry-breaking CDW order [4, 5], such as the class of recently discovered kagome materials AV<sub>3</sub>Sb<sub>5</sub> (A=K, Rb, Cs) [19–41]. Significant interests have been focused on them since an unusual competition between unconventional superconductivity and CDW order has been found [19–41]. Note that in kagome system, magnetic order and CDW order have not been usually observed simultaneously within one material, probably due to the fact that they originate from the flat band and the vHSs respectively, which have the large energy difference and usually do not both appear near the Fermi level [44].

Very recently, a CDW order has been discovered to appear deeply in a magnetically ordered kagome metal FeGe, providing the opportunity for understanding the interplay between CDW and magnetism in a kagome lattice [44–49]. Isostructural to FeSn [6–10] and CoSn [42, 43], hexagonal FeGe consists of stacks of Fe kagome planes with both in-plane and inter-plane Ge atoms [50]. A sequence of magnetic phase transitions have been discussed in 1970-80s [51-56]. Below  $T_N = 410 \text{ K}$ , FeGe exhibits collinear A-type antiferromagnetic (AFM) order with moments aligned ferromagnetically (FM) within each plane and anti-aligned between layers, and becomes a c-axis double cone AFM structure at a lower temperature  $T_{canting} = 60 \text{ K } [55, 56]$ . Recent neutron scattering, spectroscopy and transport measurements suggest a CDW in FeGe which takes place at  $T_{CDW}$  around 100K, providing the first example of a CDW in a kagome magnet [45, 46]. The CDW in FeGe enhances the AFM ordered moment and induces an emergent anomalous Hall effect (AHE) possibly associated with a chiral flux phase similar with AV<sub>3</sub>Sb<sub>5</sub> [34–36], suggesting an intimate correlation between spin, charge, and lattice degree of freedom [45]. Though AHE is not usually seen in antiferro-

<sup>\*</sup> These authors contributed equally to this work.

<sup>†</sup> Corresponding author: diwang0214@nju.edu.cn

magnets in zero field, recent studies have shown that a breaking of combined time-reversal and lattice symmetries in the antiferromagnetic state results in the AHE [57–59]. In kagome FeGe, the AHE associated with CDW order indicates that, the combined symmetry breaking occurs via the structural distortion or magnetic structure transition below the CDW temperature. The CDW in FeGe was then extensively studied experimentally and theoretically [44–49], and the CDW wavevectors are identical to that of AV<sub>3</sub>Sb<sub>5</sub> [23–28]. However, sharply different from AV<sub>3</sub>Sb<sub>5</sub> [39-41], all the theoretically calculated phonon frequencies in FeGe remain positive [44, 48, 49], and the structural distortion of the CDW phase remain elusive. It is firstly suggested to be reduced to P622with the distortion of two non-equivalent Fe atoms [45], while the later works propose that FeGe shares the same space group of P6/mmm with the pristine phase [48, 49]. Based on first-principles calculations and scanning tunneling microscopy, Shao et al. show that the CDW phase of FeGe exhibits a generalized Kekulé distortion [60] in the Ge honeycomb atomic layers [48]. Meanwhile, using hard x-ray diffraction and spectroscopy, Miao et al. report an experimental discovery of charge dimerization that coexists with the CDW phase in FeGe [49]. Therefore, the understanding of the magnetism, and the intertwined connection between complex magnetism and structural distortion in kagome FeGe is an emergency issue, which we will address in this work based on firstprinciples study and symmetry analysis.

In this work, we systematically analyze the electronic and magnetic properties of kagome FeGe. merical results show that this material is a magnetic metal exhibiting large magnetic splitting around 1.8 eV. Based on combining magnetic force theorem and linearresponse approach [61–63], the magnetic exchange parameters have been estimated. The results show that the nearest-neighbor  $J_1$  is FM and dominates over the others, while the magnetic interactions between nearest kagome layers favors AFM, consequently resulting in the A-type AFM ground-state configuration. Based on these spin exchange parameters, the calculated Néel temperature and Curie-Weiss temperature also agree well with the experiments. Using the method in Ref. [64, 65], we also calculate the magnetic anisotropic energy (MAE) to be around 0.066 meV per Fe atom with easy axis being out of the kagome layers, which is in reasonable agreement with the experimental results [56]. However, the double cone magnetic transition at  $T_{canting} = 60 \text{ K}$  cannot be reproduced by these reasonable magnetic parameters. We find that Dzyaloshinskii-Moriya (DM) interactions [66, 67] are much more efficient than Heisenberg interactions for causing this canted spin structure. Unfortunately, the space group P6/mmm of high-temperature phase in FeGe has inversion symmetry and mirror symmetries, and all of them eliminate the net contribution of DM interactions to the double cone magnetic structure. It is well known that DM interactions are very sensitive to atomic displacements, while small structural

distortion usually has little effect on Heisenberg interactions. Therefore we explore the possible CDW distortions which can explain the low-temperature magnetic structure. Symmetry theoretical analysis reveals that there are 68 different distortions, which are the subgroups of the parent P6/mmm phase with  $2\times2\times2$  supercell [45, 46, 48, 49]. Based on the group theoretical analysis, we find that only four structures (space groups P622 and  $P6_322$ ) without inversion and mirror symmetry thus can have double cone spin structure. We further propose that using Raman spectroscopy, these four CDW phases can be identified from their different numbers of Raman active peaks.

#### II. METHOD

The first-principles calculations have been carried out by using the full potential linearized augmented planewave method as implemented in the Wien2k package [68]. The converged k-point Monkhorst-Pack meshes are used for the calculations depending on materials. The self-consistent calculations are considered to be converged when the difference in the total energy of the crystal does not exceed 0.01mRy. We adopt local spin-density approximation (LSDA) [69] as the exchange-correlation potential, and include the spin orbit coupling (SOC) using the second-order variational procedure [70].

The spin exchange interactions, including Heisenberg and DM interactions [66, 67], are calculated using first principles based on combining magnetic force theorem and linear-response approach [61–63], which have successfully applied to various magnetic materials [62, 63, 71–73].

Monte Carlo (MC) simulations are performed with Metropolis algorithm for Heisenberg model [74–76]. The size of the cell in the MC simulation are  $16\times16\times16$ -unit cells with periodic boundary conditions. At each temperature we carry out 400000 sweeps to prepare the system, and sample averages are accumulated over 800000 sweeps.

#### III. RESULTS

## A. The electronic and magnetic properties

The pristine phase of FeGe crystallizes in the hexagonal structure with space group P6/mmm (No. 191) [50], where the coordinates of the atoms are shown in table II and Fig. 1. Firstly we perform nonmagnetic local-density approximation (LDA) + SOC calculation, and show the band structures in Fig. 2(a). While Ge-2p states are mainly located between -6.0 and -2.0 eV, the main contribution around the Fermi level comes from the 3d orbitals of Fe ions, as shown in Fig. 4 of Appendix. Consistent with previous first-principle calculations [44, 47], the kagome flat bands around the Fermi level exhibit a large

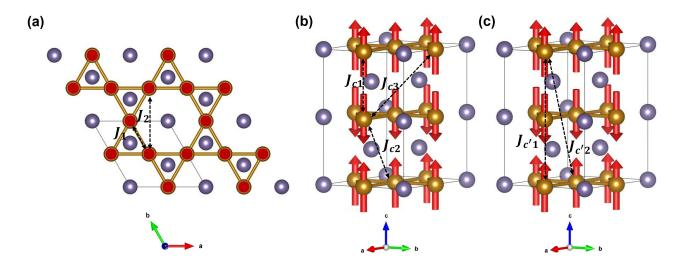


FIG. 1. Crystal and magnetic structures of FeGe. Yellow and purple spheres represent Fe and Ge atoms respectively, while arrows denote magnetic moments of Fe atoms. (a) Top view of FeGe. The exchange interactions  $J_i$  denote the *i*th-nearest-neighbor interactions between Fe ions within kagome layers. (b) The exchange interactions  $J_{ci}$  denote the *i*th-nearest-neighbor interactions between Fe ions on the nearest kagome layers. (c) The exchange interactions  $J_{c'i}$  denote the *i*th-nearest-neighbor interactions between Fe ions on the next nearest kagome layers.

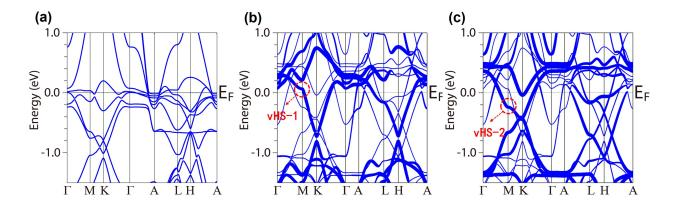


FIG. 2. (a) Band structure of nonmagnetic FeGe from LDA + SOC calculation. (b),(c) Orbital-resolved band structure of Fe- $d_{xy}/d_{x^2-y^2}$  and Fe- $d_{xz}/d_{yz}$  for A-type AFM configuration with spin orientations along the (001) direction from LSDA + SOC calculation.

peak in the density of states, which indicates the magnetic instability. Therefore, LSDA + SOC calculations are performed based on the A-type AFM configuration and the band structures are shown in Figs. 2(b) and 2(c). The magnetic moment of Fe ions is estimated to be 1.55  $\mu_B$ , which is in agreement with the previous experimental value around 1.7  $\mu_B$  [52, 54]. Note that each kagome layer is FM and the key signatures of electronic structures in kagome lattice are remained. The magnetic splitting is around 1.8 eV (see Fig. 4 of Appendix), which makes that the flat bands above and below Fermi level correspond to the spin minority bands and spin majority bands respectively. Meanwhile, the vHSs that are relatively far from the Fermi level in the nonmagnetic state, are brought near the Fermi level by the spin splitting, as

shown in Figs. 2(b) and 2(c). We present orbital-resolved band structures, and find that the vHSs near the Fermi level, which marked as vHS-1 and vHS-2 in Figs. 2(b) and 2(c), are mainly contributed by the  $d_{xy}/d_{x^2-y^2}$  and  $d_{xz}/d_{yz}$  orbitals respectively. These vHSs near the Fermi level are suggested to induce symmetry-breaking CDW order in kagome metal FeGe [44].

To quantitatively understand the rich magnetic phenomenon in kagome FeGe, a microscopic magnetic model with proper parameters is extremely important. Based on the calculated electronic structures, we estimate the exchange parameters including Heisenberg and DM interactions using the linear-response approach [61–63] and summarize the results in table I. As shown in Fig. 1, we divide the magnetic interactions considered into three

TABLE I. Spin exchange parameters (in meV) including Heisenberg and DM interactions of FeGe evaluated from LSDA+SOC calculations, respectively. The Fe-Fe distances and the corresponding number of neighbors NN are presented in the second and third columns.

	Distance(Å)	NN	J	DM
$\overline{J_1}$	2.50	4	-41.97	(0, 0, 0.03)
$J_2$	4.33	4	5.49	(0, 0, -0.12)
$J_{c1}$	4.05	2	8.44	(0, 0, 0)
$J_{c2}$	4.76	8	-2.04	(0.01, -0.02, -0.07)
$J_{c3}$	5.93	8	1.81	(0.07, -0.04, -0.09)
$J_{c'1}$	8.11	2	-0.66	(0, 0, 0)
$J_{c'2}$	8.49	8	0.09	(-0.04, -0.09, -0.03)

types: the exchange interactions  $J_i$ ,  $J_{ci}$  and  $J_{c'i}$  represent the ith-nearest-neighbor interactions between Fe ions within kagome layers, on the nearest kagome layers, and on the next nearest kagome layers respectively. As shown in table I, the in-plane nearest neighbor coupling  $J_1$ favors FM order and is estimated to be -41.97 meV, which has the similar value with the one in kagome FeSn (around -50 meV) [7–10]. Note that the distance in  $J_1$  is 2.5 Å while the others are all greater than 4 Å. Though there are also AFM in-plane magnetic interactions such as in-plane next-nearest neighbor coupling  $J_2$ , they are at least an order of magnitude smaller than  $J_1$ , resulting in each FM kagome layer. As the out-of-plane nearest neighbor coupling,  $J_{c1}$  is estimated to be 8.44 meV. It makes the magnetic moments stacked antiferromagnetically between kagome layers, consequently resulting in the A-type AFM order in kagome FeGe, which is consistent with the experiment [51]. It is worth mentioning that, SOC always exists and leads to the DM interactions even in the centrosymmetric compound FeGe, since not all Fe-Fe bonds have inversion symmetry. For the equivalent DM interactions connected by the crystal symmetry (see table III-V in Appendix), we only present one of them as a representative. As shown in table I, the inplane nearest neighbor  $\mathbf{D}_1$  has the form of  $(0, 0, D_1^z)$ according to the crystal symmetry, and  $D_1^z$  is estimated to be 0.03 meV. Meanwhile, the in-plane next nearest neighbor  $\mathbf{D}_2$  is estimated to be (0, 0, -0.12) meV. For the out-of-plane nearest neighbor,  $\mathbf{D}_{c1}$  is zero because its bond has an inversion center. The other calculated DM interactions are also listed in table I, and most of them are small in the order of 0.01 meV.

To explore the magnetic anisotropy in kagome FeGe, we consider the MAE with the expression  $E_{MAE}=K_2\sin^2\theta+K_4\sin^4\theta$  [51, 54–56] neglecting terms of order higher than four, where  $\theta$  is the angle between the magnetic moment and the z-axis. The values of  $K_2$  and  $K_4$  are estimated to be 0.066 meV and 0.018 meV respectively based on the approach of Ref. [64, 65], which are in reasonable agreement with the experimental values 0.021 meV [56] and 0.012 meV [51]. Here  $K_2$  and  $K_4$  are both positive, making out-of-plane magnetization favored, which is different from the easy-plane anisotropy

in FeSn [8]. Note that positive  $K_4$  is the requirement for the stability of the double cone magnetic structure, which will be discussed below.

According to the experiments [51], the Curie-Weiss temperature  $\theta_{CW}$  in kagome FeGe is -200 K while the Néel temperature  $T_N$  is 410 K. The relative low value of the frustration index  $|\theta_{CW}|/T_N$  (smaller than 1) reveals the interplay of the FM and AFM interactions [77]. As shown in table I, our calculated results of spin exchange couplings also verify the coexistence of the FM and AFM interactions. Based on these calculated spin exchange parameters, we calculate Néel temperature and Curie-Weiss temperature by MC simulations [74–76]. The  $\theta_{CW}$  and  $T_N$  are calculated to be -219 K and 370 K respectively, which agrees well with the experiment [51].

Similar to the electronic structure of a kagome lattice, the spin wave for a localized spin model with FM nearestneighbor magnetic exchange also yields a flat magnetic band and a Dirac magnon [78]. Using the calculated spin model parameters, one can obtain the magnon spectrum [79, 80]. The calculated spin-wave dispersion along the high-symmetry axis is shown in Fig. 3, which basically captures the key features of kagome lattice geometry. Similar with FeSn case [7–10], strongly dispersive magnons in the xy-plane extend to about 260 meV, where the magnon dispersion along the out-of-plane direction has relatively small bandwidth of less than 15 meV, reflecting the quasi-two-dimensional magnetic properties in kagome FeGe. Meanwhile, the Dirac-like node appears at the K point at about 107 meV, and we find that DM interactions introduce a gap around 1 meV at the Dirac point, as shown in the inset of Fig. 3. Furthermore, the single-ion anisotropy produces a spin gap of about 2 meV, which could be verified in future inelastic neutron scattering experiments.

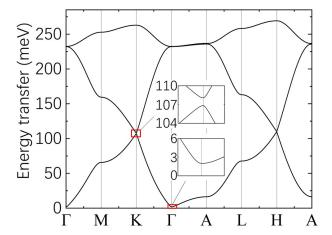


FIG. 3. Calculated spin-wave dispersion curves along the high-symmetry axis for FeGe. The insets show the spin gap at  $\Gamma$  point induced by easy-axis anisotropy, and the gap located at about 107 meV of K point induced by DM interactions.

#### B. The double cone magnetic structure

At  $T_{canting}=60$  K, the kagome lattice FeGe becomes a c-axis double cone AFM structure [51, 52, 54–56] where the magnetic ground state could be written as Eq. (10) in Appendix. Considering the magnetic interactions and the MAE, the total energy of the double cone spin structure could be written as Eq. (12) in Appendix. When DM interactions are not considered, the extremum condition of the total energy gives the equilibrium value of wave vector  $\delta$  and the cone half angle  $\theta$  (i.e. Eq. (13) and (14) in Appendix)

$$\cos \delta = \frac{\sum_{i} N_{ci} J_{ci}}{4 \sum_{i} N_{c'i} J_{c'i}} \tag{1}$$

$$\sin^2 \theta = -\frac{K_2 - \frac{1}{2N} \sum_i N_{c'i} J_{c'i} \delta^4}{2K_4}$$
 (2)

Note that the minimum of the total energy requires that the second derivative of Eq. (12) in Appendix is positive, thus  $K_4$  must be positive. Hence  $K_2 - \frac{1}{2N} \sum_i N_{c'i} J_{c'i} \delta^4$  (i.e. the numerator of Eq. (2)) must be negative. However, our reasonable magnetic parameters cannot explain the double cone magnetic ground state. The value of wave vector  $\delta$  is small in experimental measurement (0.17 in Ref. [51] and 0.25 in Ref. [53]), thus  $\delta^4$  is around 0.001. Meanwhile, the value of  $\frac{1}{2N} \sum_i N_{c'i} J_{c'i}$  is of the order of 1 meV, which obviously cannot explain the double cone magnetic structure [51].

We thus consider the effect of DM interactions on double cone spin structure. Since the exchange interactions between two next nearest neighbor kagome layers are relatively small, we only consider the Heisenberg and DM interactions between two nearest neighbor kagome layers, i.e.  $J_{ci}$  and  $\mathbf{D}_{ci}$ . We find that wave vector  $\delta$  and the cone half angle  $\theta$  have the expressions as (i.e. Eq. (15) and (16) in Appendix)

$$\tan \delta = \frac{\sum_{i,j} D_{ci,j}^z}{\sum_i N_{ci} J_{ci}} \tag{3}$$

$$\sin^2 \theta = -\frac{K_2 - \frac{1}{2N} \sum_{i,j} D_{ci,j}^z \delta}{2K_4}$$
 (4)

It should be noted that, comparing Eq. (2) and (4), DM interactions are more efficient than Heisenberg interactions for causing double cone spin structure since  $\delta$  is small. Though the space group P6/mmm of high-temperature phase in FeGe has a global inversion center, not all Fe-Fe bonds have inversion symmetry and DM interactions could exist. However, according to the inversion symmetry of space group P6/mmm, the total contribution of DM interactions to the energy of double cone magnetic structure in Eq. (12) is absent, i.e.  $\sum_{i,j} D_{ci,j}^z = 0$  (see Appendix D). Meanwhile, mirror symmetries in space group P6/mmm would also eliminate the contribution of DM interactions based on the

symmetry analysis. Therefore, DM interactions have no net contribution to double cone magnetic structure with the symmetry of high-temperature phase. For the CDW phases with the space group of P6/mmm suggested by Ref. [48, 49] (the first two structures of the table VI in Appendix), the total contribution of DM interactions is still absent and cannot explain the magnetic ground state of double cone spin structure.

# C. The interplay of CDW and double cone structure

As mentioned above, DM interactions play a more important role in the double cone spin structure. Meanwhile, it is very sensitive to atomic displacements. Therefore, in the following we explore the CDW phases with symmetry-allowed DM contribution to double cone spin structure which may explain the canted magnetic ground state.

The  $2 \times 2 \times 2$  supercell structure of CDW phase (compared with the nonmagnetic pristine phase) is suggested experimentally [45, 46, 48, 49]. Considering all CDW phases whose associated point group in the maximal subgroups of  $D_{6h}$ , we find 68 different possible CDW phases which are the subgroups of the parent P6/mmm phase with  $2 \times 2 \times 2$  supercell (see details in Appendix D). The corresponding relations of atomic positions between the pristine phase and these proposed CDW phases are all summarized in table VI-X of Appendix.

Note that the inversion symmetry and mirror symmetries would all eliminate the net contribution of DM interactions as disscussed above. We find that among these 68 proposed CDW phases, only four distorted structures break all these symetries above, and can lead to non-zero DM contribution in Eq. (12) of Appendix. We list the corresponding Wyckoff positions (WP) and the coordinates of the atoms in the pristine phase and these four CDW phases in table II. They comes from two space groups P622 and  $P6_322$ . It should be mentioned that there are two different CDW phases for each of these two space groups, which are labeled as (type I) and (type II) in table II. Note that the CDW phase with P622 space group is also suggested in Ref. [45].

Raman spectroscopy is a fast and usually non-destructive technique which can be used to characterize the structural distortion of materials. Based on the atomic coordinates in table II, we predict the irreducible representation of the Raman active modes of these four proposed CDW phases using symmetry analysis [81]. For P622 (type I) and (type II) CDW phases, the Raman active modes are  $8A_1 + 26E_1 + 22E_2$  and  $10A_1 + 26E_1 + 22E_2$ . Meanwhile, for  $P6_322$  (type I) and (type II), the Raman active modes are  $8A_1 + 24E_1 + 24E_2$  and  $10A_1 + 24E_1 + 24E_2$ , respectively. Note that even within the same symmetry of space group P622, the different structural distortion of CDW phases P622 (type I) and (type II) could result in the different number of Raman active

TABLE II. Four	pes of $2 \times 2 \times 2$ CDW phases which can lead to non-zero DM contribution to double cone spin st	tructure.
The corresponding	Wyckoff positions and the coordinates of the atoms in the pristine phase and these four CDW ph	hases are
summarized.		

				2(type I)		P62	2(type II)		$P6_3$	22(type I)	$P6_322$ (type II)			
	WP	Coordinates		WP	Coordinates		WP	Coordinates		WP	Coordinates		WP	Coordinates
			Ge1	1a	(0, 0, 0)	Ge1	2e	$(0, 0, z_1)$	Ge1	2a	(0, 0, 0)	Ge1	2b	(0, 0, 1/4)
Ge1	1a	(0, 0, 0)	Ge2	1b	(0, 0, 1/2)	Ge2	6i	$(1/2, 0, z_2)$	Ge2	6g	$(x_1, 0, 0)$	Ge2	6h	$(x_1, 2x_1, 1/4)$
Ger	1a	(0,  0,  0)	Ge3	3f	(0, 1/2, 0)									
			Ge4	3g	(0, 1/2, 1/2)									
			Ge5	4h	$(1/3, 2/3, z_1)$	Ge3	2c	(1/3, 2/3, 0)	Ge3	2c	(1/3, 2/3, 1/4)	Ge3	4f	$(1/3, 2/3, z_2)$
Ge2	24	(1/3, 2/3, 1/2)	Ge6	12n	$(x_2, y_2, z_2)$	Ge4	2d	(1/3, 2/3, 1/2)	Ge4	2d	(1/3, 2/3, 3/4)	Ge4	12i	$(x_3, y_3, z_3)$
Gez	2 <b>u</b>	(1/3, 2/3, 1/2)				Ge5	6l	$(x_3, 2x_3, 0)$	Ge5	6h	$(x_2, 2x_2, 1/4)$			
						Ge6	$6 \mathrm{m}$	$(x_4, 2x_4, 1/2)$	Ge6	6h	$(x_3, 2x_3, 1/4)$			
			Fe1	6j	$(x_3, 0, 0)$	Fe1	12n	$(x_5, y_5, z_5)$	Fe1	6g	$(x_4, 0, 0)$	Fe1	6h	$(x_4, 2x_4, 1/4)$
Fe	3f	(1/2, 0, 0)	Fe2	6k	$(x_4, 0, 1/2)$	Fe2	12n	$(x_6, y_6, z_6)$	Fe2	6g	$(x_5, 0, 0)$	Fe2	6h	$(x_5, 2x_5, 1/4)$
те	91	(1/2, 0, 0)	Fe3	6l	$(x_5, 2x_5, 0)$				Fe3	12i	$(x_6, y_6, z_6)$	Fe3	12i	$(x_6, y_6, z_6)$
			Fe4	$6 \mathrm{m}$	$(x_6, 2x_6, 1/2)$									

modes (56 and 58 respectively), which could be identified by Raman spectroscopy.

#### IV. CONCLUSION

In conclusion, we systematically analyze the electronic and magnetic properties of kagome FeGe. Our numerical results show that this material is a magnetic metal exhibiting large magnetic splitting around 1.8 eV. The magnetic splitting makes the flat bands away from Fermi level, and bring two vHSs near the Fermi level. We estimate the magnetic parameters, and find that the ferromagnetic nearest-neighbor  $J_1$  dominates over the others, while the magnetic interactions between nearest kagome layers favors antiferromagnetic. Based on these spin exchange parameters, the calculated Néel temperature and Curie-Weiss temperature also agree well with the experiments. Furthermore, the magnetic excitation spectra are calculated using linear spin wave theory and a spin gap about 2 meV is predicted. Note that the double cone magnetic transition at a lower temperature cannot be reproduced by these reasonable magnetic parameters. Meanwhile, due to the inversion symmetry and mirror symmetries in the space group P6/mmm of hightemperature phase, the total contribution of DM interactions to the double cone magnetic structure is absent. Since DM interactions are very sensitive to small atomic displacements and symmetry restrictions, and also much more efficient than Heisenberg interactions for causing this canted spin structure, we propose that the double cone spin structure may arise from the structural distortion. We explore 68 possible CDW phases of kagome FeGe which are subgroups of the pristine phase with  $2 \times 2 \times 2$  supercell, and symmetry-allowed four CDW structures which have non-zero DM contribution and may result in double cone spin structure are proposed. These four CDW phases belong to two space groups P622 and P6<sub>3</sub>22, and we further propose that they can

be identified from their different numbers of Raman active peaks. Therefore, we believe that symmetry analysis plays an important role in exploring the possible structural distortion in complex magnetic configurations.

#### V. ACKNOWLEDGEMENTS

This work was supported by the NSFC (No. 12188101, 11834006, 12004170, 11790311, 51721001), National Key R&D Program of China (No. 2018YFA0305704), Natural Science Foundation of Jiangsu Province, China (Grant No. BK20200326), and the excellent programme in Nanjing University. Xiangang Wan also acknowledges the support from the Tencent Foundation through the XPLORER PRIZE.

# VI. APPENDIX

#### A. The density of states in kagome FeGe

The Partial density of states (DOS) of FeGe from LSDA + SOC calculations are shown in Fig. 4.

# B. The symmetry restrictions on the magnetic interactions

Here we consider a general pairwise spin model

$$H = \sum_{l,n,l',n'} \mathbf{S}_{ln} \mathbf{J}_{\mathbf{R}_l + \boldsymbol{\tau}_n, \mathbf{R}_{l'} + \boldsymbol{\tau}_{n'}} \mathbf{S}_{l'n'}$$
 (5)

where  $\mathbf{J}_{\mathbf{R}_l+\boldsymbol{\tau}_n,\mathbf{R}_{l'}+\boldsymbol{\tau}_{n'}}$ , a 3 × 3 tensor, represents the spin exchange parameters.  $\mathbf{R}_l$  and  $\boldsymbol{\tau}_n$  represent the lattice translation vector and the position of magnetic ions in the lattice basis, and  $\mathbf{S}_{ln}$  means the spin at the site of  $\mathbf{R}_l + \boldsymbol{\tau}_n$ . Translation symmetry will restrict

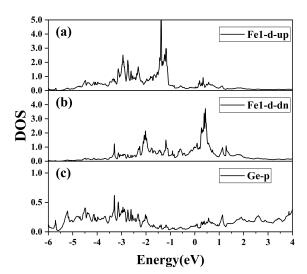


FIG. 4. Partial DOS of FeGe from LSDA + SOC calculations. The Fermi energy is set to zero. (a) and (b) represent the spinup and spin-down channel of d orbitals in Fe1 atom located at (1/2,0,0), while (c) represents the DOS of Ge-p orbitals.

TABLE III. The distances, the bond information and the symmetry restricted interactions of corresponding Fe ions within xy-planes. Here n, n' and  $R_l$  correspond to  $\mathbf{J}_{\boldsymbol{\tau}_n, \boldsymbol{\tau}_{n'} + \mathbf{R}_l}$ , where  $R_l$  and  $\tau_n$  represent the lattice translation vector and the position of magnetic ions in the lattice basis. Three magnetic ions are located at  $\tau_1$  (1/2, 0, 0),  $\tau_2$  (0, 1/2, 0), and  $\tau_3$  (1/2, 1/2, 0). The equivalent  $\mathbf{D}_i$ 's are labeled as the sub-index of j, i.e. the  $\mathbf{D}_{i,j}$  in the table.

Distance(Å)	n	n'	$R_l$	J	DM
2.50	3	1	(0,1,0)	$J_1$	$\mathbf{D}_{1,1}(0,0,D_1^z)$
	1	2	(0,-1,0)	$J_1$	$\mathbf{D}_{1,2}(0,0,D_1^z)$
	2	3	(0,0,0)	$J_1$	$\mathbf{D}_{1,3}(0,0,D_1^z)$
	3	1	(0,0,0)	$J_1$	$\mathbf{D}_{1,4}(0,0,D_1^z)$
	1	2	(1,0,0)	$J_1$	$\mathbf{D}_{1,5}(0,0,D_1^z)$
	2	3	(-1,0,0)	$J_1$	$\mathbf{D}_{1,6}(0,0,D_1^z)$
4.33	1	2	(1,-1,0)	$J_2$	$\mathbf{D}_{2,1}(0,0,D_2^z)$
	2	3	(0,1,0)	$J_2$	$\mathbf{D}_{2,2}(0,0,D_2^z)$
	3	1	(-1,0,0)	$J_2$	$\mathbf{D}_{2,3}(0,0,D_2^z)$
	1	2	(0,0,0)	$J_2$	$\mathbf{D}_{2,4}(0,0,D_2^z)$
	2	3	(-1,-1,0)	$J_2$	$\mathbf{D}_{2,5}(0,0,D_2^z)$
	3	1	(1,1,0)	$J_2$	$\mathbf{D}_{2,6}(0,0,D_2^z)$

 $\mathbf{J}_{\mathbf{R}_l+\boldsymbol{\tau}_n,\mathbf{R}_{l'}+\boldsymbol{\tau}_{n'}}$  to be only related to  $\mathbf{J}_{\boldsymbol{\tau}_n,\boldsymbol{\tau}_{n'}+\mathbf{R}_{l''}}$  where  $R_{l''}=R_{l'}-R_l$ , irrespective of the starting unit cell. Other spatial symmetries will also give restrictions on the magnetic exchange interactions. We consider a general space group element  $\{\alpha|\mathbf{t}\}$ , where the left part represents the rotation and the right part means the lattice translation. Supposing under this symmetry operator,  $\mathbf{R}_m+\boldsymbol{\tau}_p$  and  $\mathbf{R}_{m'}+\boldsymbol{\tau}_{p'}$  transfer to  $\mathbf{R}_l+\boldsymbol{\tau}_n$  and  $\mathbf{R}_{l'}+\boldsymbol{\tau}_{n'}$ , re-

TABLE IV. The distances, the bond information and the symmetry restricted interactions of corresponding Fe ions between nearest-neighbor (001)-planes. Here n, n' and  $R_l$  correspond to  $\mathbf{J}_{\boldsymbol{\tau}n,\boldsymbol{\tau}_{\boldsymbol{n'}}+\mathbf{R}_l}$ , where  $R_l$  and  $\tau_n$  represent the lattice translation vector and the position of magnetic ions in the lattice basis. Three magnetic ions are located at  $\tau_1$  (1/2, 0, 0),  $\tau_2$  (0, 1/2, 0), and  $\tau_3$  (1/2, 1/2, 0). The equivalent  $\mathbf{D}_{ci}$ 's are labeled as the sub-index of j, i.e. the  $\mathbf{D}_{ci,j}$  in the table.

			1 3, 110. 01		et,j ili tilo tasio.
Distance(Å)	n	n'		J	DM
4.05	1	1	(0,0,1)	$J_{c1}$	$\mathbf{D}_{c1,1}(0,0,0)$
	2	$^{2}$	(0,0,1)	$J_{c1}$	$\mathbf{D}_{c1,2}(0,0,0)$
	3	3	(0,0,1)	$J_{c1}$	$\mathbf{D}_{c1,3}(0,0,0)$
4.76	3	1	(0,0,1)	$J_{c2}$	$\mathbf{D}_{c2,1}(D_{c2}^x, -\sqrt{3}D_{c2}^x, D_{c2}^z)$
	1	2	(1,0,1)	$J_{c2}$	$\mathbf{D}_{c2,2}(D_{c2}^x, \sqrt{3}D_{c2}^x, D_{c2}^z)$
	2	3	(-1,0,1)	$J_{c2}$	$\mathbf{D}_{c2,3}(-2D_{c2}^x, 0, D_{c2}^z)$
	3	1	(0,1,1)	$J_{c2}$	$\mathbf{D}_{c2,4}(-D_{c2}^x, \sqrt{3}D_{c2}^x, D_{c2}^z)$
	1	2	(0,-1,1)	$J_{c2}$	$\mathbf{D}_{c2,5}(-D_{c2}^x, -\sqrt{3}D_{c2}^x, D_{c2}^z)$
	2	3	(0,0,1)	$J_{c2}$	$\mathbf{D}_{c2,6}(2D_{c2}^x, 0, D_{c2}^z)$
	1	3	(0,-1,1)	$J_{c2}$	$\mathbf{D}_{c2,7}(-D_{c2}^x,\sqrt{3}D_{c2}^x,-D_{c2}^z)$
	2	1	(0,1,1)	$J_{c2}$	$\mathbf{D}_{c2,8}(-D_{c2}^x, -\sqrt{3}D_{c2}^x, -D_{c2}^z)$
	3	$^{2}$	(0,0,1)	$J_{c2}$	$\mathbf{D}_{c2,9}(2D_{c2}^x, 0, -D_{c2}^z)$
	1	3	(0,0,1)	$J_{c2}$	$\mathbf{D}_{c2,10}(D_{c2}^x, -\sqrt{3}D_{c2}^x, -D_{c2}^z)$
	2	1	(-1,0,1)	$J_{c2}$	$\mathbf{D}_{c2,11}(D_{c2}^x, \sqrt{3}D_{c2}^x, -D_{c2}^z)$
	3	2	(1,0,1)	$J_{c2}$	$\mathbf{D}_{c2,12}(-2D_{c2}^x, 0, -D_{c2}^z)$
5.93	2	1	(-1,1,1)	$J_{c3}$	$\mathbf{D}_{c3,1}(-\sqrt{3}D_{c3}^y, D_{c3}^y, -D_{c3}^z)$
	3	2	(0,-1,1)	$J_{c3}$	$\mathbf{D}_{c3,2}(0, -2D_{c3}^y, -D_{c3}^z)$
	1	3	(1,0,1)	$J_{c3}$	
	2	1	(0,0,1)	$J_{c3}$	$\mathbf{D}_{c3,4}(\sqrt{3}D_{c3}^y, -D_{c3}^y, -D_{c3}^z)$
	3	2	(1,1,1)	$J_{c3}$	$\mathbf{D}_{c3,5}(0,2D_{c3}^y,-D_{c3}^z)$
	1	3	(-1,-1,1)	$J_{c3}$	$\mathbf{D}_{c3,6}(-\sqrt{3}D_{c3}^y, -D_{c3}^y, -D_{c3}^z)$
	1	2	(0,0,1)	$J_{c3}$	$\mathbf{D}_{c3,7}(\sqrt{3}D_{c3}^y, -D_{c3}^y, D_{c3}^z)$
	2	3	(-1,-1,1)	$J_{c3}$	$\mathbf{D}_{c3,8}(0,2D_{c3}^y,D_{c3}^z)$
	3	1	(1,1,1)	$J_{c3}$	$\mathbf{D}_{c3,9}(-\sqrt{3}D_{c3}^y, -D_{c3}^y, D_{c3}^z)$
	1	2	(1,-1,1)	$J_{c3}$	$\mathbf{D}_{c3,10}(-\sqrt{3}D_{c3}^y, D_{c3}^y, D_{c3}^z)$
	2	3	(0,1,1)	$J_{c3}$	$\mathbf{D}_{c3,11}(0, -2D_{c3}^y, D_{c3}^z)$
	3	1	(-1,0,1)	$J_{c3}$	$\mathbf{D}_{c3,12}(\sqrt{3}D_{c3}^y, D_{c3}^y, D_{c3}^z)$

spectively, meanwhile the transformation of spin becomes  $\mathbf{S}_{mp} = M(\alpha)\mathbf{S}_{ln}$ , where  $M(\alpha)$  is the representation matrix of the proper rotation part of the operation  $\alpha$  in the coordinate system, we get the following expression:

$$H = \sum_{l,n,l',n'} \mathbf{S}_{ln} \mathbf{J}_{\mathbf{R}_{l}+\boldsymbol{\tau}_{n},\mathbf{R}_{l'}+\boldsymbol{\tau}_{n'}} \mathbf{S}_{l'n'}$$

$$= \sum_{l,n,l',n'} \mathbf{S}_{ln} M^{\dagger}(\alpha) M(\alpha) \mathbf{J}_{\mathbf{R}_{l}+\boldsymbol{\tau}_{n},\mathbf{R}_{l'}+\boldsymbol{\tau}_{n'}} M^{\dagger}(\alpha) M(\alpha) \mathbf{S}_{l'n'}$$

$$= \sum_{m,p,m',p'} \mathbf{S}_{mp} \left[ M(\alpha) \mathbf{J}_{\mathbf{R}_{l}+\boldsymbol{\tau}_{n},\mathbf{R}_{l'}+\boldsymbol{\tau}_{n'}} M^{\dagger}(\alpha) \right] \mathbf{S}_{m'p'}$$
(6)

Then the exchange interactions should satisfy the following condition:

$$\mathbf{J}_{\mathbf{R}_{m}+\boldsymbol{\tau}_{n},\mathbf{R}_{m'}+\boldsymbol{\tau}_{n'}} = M(\alpha)\mathbf{J}_{\mathbf{R}_{l}+\boldsymbol{\tau}_{n},\mathbf{R}_{l'}+\boldsymbol{\tau}_{n'}}M^{\dagger}(\alpha) \quad (7)$$

After decomposing the  $3\times3$  tensor **J** into scalar Heisenberg term J and vector DM term **D** as in the maintext, we obtain the following results:

TABLE V. The distances, the bond information and the symmetry restricted interactions of corresponding Fe ions between next-nearest-neighbor (001)-planes. Here n, n' and  $R_l$  correspond to  $\mathbf{J}_{\boldsymbol{\tau}n,\boldsymbol{\tau}_{\boldsymbol{n'}}+\mathbf{R}_l}$ , where  $R_l$  and  $\boldsymbol{\tau}_n$  represent the lattice translation vector and the position of magnetic ions in the lattice basis. Three magnetic ions are located at  $\tau_1$  (1/2, 0, 0),  $\tau_2$  (0, 1/2, 0), and  $\tau_3$  (1/2, 1/2, 0). The equivalent  $\mathbf{D}_{c'i}$ 's are labeled as the sub-index of j, i.e. the  $\mathbf{D}_{c'i,j}$  in the table.

Distance(Å)	n	n'	$R_l$	J	DM
8.11	1	1	(0,0,2)	$J_{c'1}$	$\mathbf{D}_{c'1,1}(0,0,0)$
	2	2	(0,0,2)	$J_{c'1}$	$\mathbf{D}_{c'1,2}(0,0,0)$
	3	3	(0,0,2)	$J_{c'1}$	$\mathbf{D}_{c'1,3}(0,0,0)$
8.49	2	1	(0,1,2)	$J_{c'2}$	$\mathbf{D}_{c'2,1}(D^x_{c'2}, \sqrt{3}D^x_{c'2}, D^z_{c'2})$
	3	2	(0,0,2)	$J_{c'2}$	$\mathbf{D}_{c'2,2}(-2D_{c'2}^x, 0, D_{c'2}^z)$
	1	3	(0,-1,2)	$J_{c'2}$	$\mathbf{D}_{c'2,3}(D_{c'2}^x, -\sqrt{3}D_{c'2}^x, D_{c'2}^z)$
	2	1	(-1,0,2)	$J_{c'2}$	$\mathbf{D}_{c'2,4}(-D_{c'2}^x, -\sqrt{3}D_{c'2}^x, D_{c'2}^z)$
	3	2	(1,0,2)	$J_{c'2}$	$\mathbf{D}_{c'2,5}(2D_{c'2}^x, 0, D_{c'2}^z)$
	1	3	(0,0,2)		$\mathbf{D}_{c'2,6}(-D_{c'2}^x,\sqrt{3}D_{c'2}^x,D_{c'2}^z)$
	1	2	(1,0,2)	$J_{c'2}$	$\mathbf{D}_{c'2,7}(-D_{c'2}^x, -\sqrt{3}D_{c'2}^x, -D_{c'2}^z)$
	2	3	(-1,0,2)		$\mathbf{D}_{c'2,8}(2D_{c'2}^x, 0, -D_{c'2}^z)$
	3	1	(0,0,2)	$J_{c'2}$	$\mathbf{D}_{c'2,9}(-D_{c'2}^x, \sqrt{3}D_{c'2}^x, -D_{c'2}^z)$
	1	2	(0,-1,2)	$J_{c'2}$	$\mathbf{D}_{c'2,10}(D_{c'2}^x, \sqrt{3}D_{c'2}^x, -D_{c'2}^z)$
	2	3	(0,0,2)		$\mathbf{D}_{c'2,11}(-2D_{c'2}^x, 0, -D_{c'2}^z)$
	3	1	(0,1,2)	$J_{c'2}$	$\mathbf{D}_{c'2,12}(D_{c'2}^x, -\sqrt{3}D_{c'2}^x, -D_{c'2}^z)$

$$J_{\mathbf{R}_{m}+\boldsymbol{\tau}_{p},\mathbf{R}_{m'}+\boldsymbol{\tau}_{p'}} = J_{\mathbf{R}_{l}+\boldsymbol{\tau}_{n},\mathbf{R}_{l'}+\boldsymbol{\tau}_{n'}}$$

$$\mathbf{D}_{\mathbf{R}_{m}+\boldsymbol{\tau}_{p},\mathbf{R}_{m'}+\boldsymbol{\tau}_{n'}} = M(\alpha)\mathbf{D}_{\mathbf{R}_{l}+\boldsymbol{\tau}_{n},\mathbf{R}_{l'}+\boldsymbol{\tau}_{n'}}$$
(8)

Meanwhile, it is should be noted that the Heisenberg and DM interactions obey the following commutation relations

$$J_{\mathbf{R}_{l'}+\boldsymbol{\tau}_{n'},\mathbf{R}_{l}+\boldsymbol{\tau}_{n}} = J_{\mathbf{R}_{l}+\boldsymbol{\tau}_{n},\mathbf{R}_{l'}+\boldsymbol{\tau}_{n'}}$$

$$D_{\mathbf{R}_{l'}+\boldsymbol{\tau}_{n'},\mathbf{R}_{l}+\boldsymbol{\tau}_{n}} = -D_{\mathbf{R}_{l}+\boldsymbol{\tau}_{n},\mathbf{R}_{l'}+\boldsymbol{\tau}_{n'}}$$
(9)

According to the above equations (i.e. Eq. (8) and (9)), one can obtain the symmetry restricted magnetic interactions for kagome FeGe with space group P6/mmm, as shown in table III, IV and V. Note that the equivalent  $\mathbf{D}_{i}$ 's are labeled as the sub-index of j, i.e. the  $\mathbf{D}_{i,j}$  in table III, IV and V.

## C. The details of double cone structure

According to the experimental works [51, 54–56], in hexagonal FeGe there is a transition from a uniaxial spin system to a double cone spin structure at  $T_{canting} = 60$  K [51], which is expressed by the following equations:

$$\langle S^{x} \rangle = S \sin \theta \cos \left( (\pi \pm \delta) \frac{z}{c} + \varphi \right)$$

$$\langle S^{y} \rangle = S \sin \theta \sin \left( (\pi \pm \delta) \frac{z}{c} + \varphi \right)$$

$$\langle S^{z} \rangle = S \cos \theta \cos \left( \frac{\pi z}{c} \right)$$
(10)

where  $\theta$  is the cone half angle, and c represents the lattice parameter. If  $\delta=0$  there will be a simple tilting of the spins. When  $\delta$  represents the small angle, Eq. (10) gives a double cone spin structure. Following the previous works [51, 54–56], here we consider the MAE with the expression neglecting terms of order higher than four written as

$$E_{MAE} = K_2 \sin^2 \theta + K_4 \sin^4 \theta \tag{11}$$

Therefore the total energy of Eq. (5) and Eq. (11) in double cone spin structure per unit cell could be written as

$$E(\delta, \theta) = \sum_{i} N_{ci} J_{ci} (-\sin^2 \theta \cos \delta - \cos^2 \theta)$$

$$+ \sum_{i} N_{c'i} J_{c'i} (\sin^2 \theta \cos 2\delta + \cos^2 \theta)$$

$$- \sum_{i,j} D_{ci,j}^z (\sin^2 \theta \sin \delta)$$

$$- \sum_{i,j} D_{c'i,j}^z (\sin^2 \theta \sin 2\delta)$$

$$+ N(K_2 \sin^2 \theta + K_4 \sin^4 \theta)$$
(12)

where  $N_{ci}$  and  $N_{c'i}$  are the corresponding number of neighbors of  $J_{ci}$  and  $J_{c'i}$ , and N represents the number of magnetic ions in one unit cell. When DM interactions are not considered, the extremum condition in total energ gives the equilibrium value of wave vector  $\delta$  with following equation [51, 56]:

$$\cos \delta = \frac{\sum_{i} N_{ci} J_{ci}}{4 \sum_{i} N_{c'i} J_{c'i}} \tag{13}$$

While the cone half angle  $\theta$  has the expression as

$$\sin^2 \theta = -\frac{K_2 - \frac{1}{2N} \sum_i N_{c'i} J_{c'i} \delta^4}{2K_4}$$
 (14)

A minimum in the total energy (see Eq. (12)) will occur only if  $K_4$  is positive, and Eq. (14) requires that  $K_2 - \frac{1}{2N} \sum_i N_{c'i} J_{c'i} \delta^4$  must be negative.

When the magnetic interactions including Heisenberg and DM interactions between two nearest neighbor xyplanes, i.e.  $J_{ci}$  and  $\mathbf{D}_{ci}$ , are considered, the equilibrium value of wave vector  $\delta$  is obtained by the minimum in total energy written as

$$\tan \delta = \frac{\sum_{i,j} D_{ci,j}^z}{\sum_i N_{ci} J_{ci}} \tag{15}$$

where j is the sub-index of the equivalent  $\mathbf{D}_{ci}$ 's. Meanwhile, we find the following expression for  $\theta$ 

$$\sin^2 \theta = -\frac{K_2 - \frac{1}{2N} \sum_{i,j} D_{ci,j}^z \delta}{2K_4}$$
 (16)

Note that in Eq. (16), DM interactions are combined with only the first order of  $\delta$ , and may have much more efficient than  $J_{c'i}$  in Eq. (14) since  $\delta$  is small around 0.2 [51, 53]. This implies that DM interactions may be the origin of double cone structure.

# D. The symmetry analysis of CDW phases

The high-temperature phase FeGe crystallizes in space group P6/mmm, which has the generators  $\{3^{+}_{001}|0\}$ ,  $\{2_{001}|0\}, \{2_{110}|0\} \text{ and } \{-1|0\}, \text{ where the left part rep-}$ resents the rotation and the right part means the lattice translation (here -1 denotes the inversion symmetry). According to the inversion symmetry, the total contribution of DM interactions to the energy of double cone magnetic structure in Eq. (12) is absent, i.e.  $\sum_{i,j} D_{ci,j}^z = 0$ , which is easy to see from the table IV-V. Firstly, each kagome layer is still FM in the double cone magnetic state, thus the in-plane DM interactions are ineffective. For interlayer DM interactions with an inversion center such as  $\mathbf{D}_{c1}$ , the inversion symmetry restricts it to be zero as shown in table IV. Meanwhile, for other interlayer DM interactions, the inversion symmetry combine the equivalent DM interactions in pairs. For example, as shown in table IV, the  $\mathbf{D}_{c2,1}$  and  $\mathbf{D}_{c2,7}$  are connected by the inversion symmetry, and have opposite values. Therefore, the summation over equivalent interlayer DM interactions are all zero due to the inversion symmetry. Note that not only inversion symmetry, but mirror symmetries such as  $\{m_{001}|0\}$ ,  $\{m_{110}|0\}$ ,  $\{m_{100}|0\}$ ,  $\{m_{010}|0\}, \{m_{1-10}|0\}, \{m_{120}|0\} \text{ and } \{m_{210}|0\} \text{ in space }$ group P6/mmm, would also make the DM contribution to the canted magnetic ground state to be zero based on the similar analysis above. Therefore, DM interactions have no contribution to double cone magnetic structure with the symmetry of high-temperature phase.

As mentioned in the maintext, since the  $2 \times 2 \times 2$ supercell structure of CDW phase (compared with the nonmagnetic pristine phase) is suggested experimentally [45, 46, 48, 49], we present the possible CDW phases of kagome FeGe with  $2 \times 2 \times 2$  supercell. The  $2 \times 2 \times 2$ supercell without distortion has the symmetry of space group P6/mmm, the non-primitive translation operations  $t_x$  {1|1/2,0,0},  $t_y$  {1|0,1/2,0},  $t_z$  {1|0,0,1/2}, and many symmetry operations from their combinations. As the subgroups compatible with  $2 \times 2 \times 2$  supercell of pristine FeGe, the structural distortion of CDW phases would break the non-primitive translation operations  $t_x$ ,  $t_y$  and  $t_z$ , and possibly break other symmetry operations as well. Since the point group associated with hightemperature phase FeGe (P6/mmm) is  $D_{6h}$ , we consider all CDW phases whose associated point group is  $D_{6h}$  itself or in maximal subgroups of  $D_{6h}$  ( $D_{2h}$ ,  $D_6$ ,  $C_{6h}$ ,  $C_{6v}$ ,  $D_{3d}$ ,  $D_{3h}$ ). In total we find 68 different possible CDW phases, and list the corresponding relations of atomic positions in the high-temperature phase and all types of

proposed CDW phases in table VI-X. Note that the inversion symmetry and mirror symmetries in parent group P6/mmm would all eliminate the contribution of DM interactions based on the symmetry analysis. Among these 68 proposed CDW phases, only four distorted structures do not have the inversion symmetry and mirror symmetries, which can lead to non-zero DM contribution to double cone spin structure and may explain this magnetic ground state. They belong to two space groups P622 and  $P6_322$ , and we list the corresponding Wyckoff positions and the coordinates of the atoms in the pristine phase and these four CDW phases in table II of the maintext.

TABLE VI. The corresponding Wyckoff positions and the coordinates of the atoms in the pristine phase and CDW phases with different symmetries. (PART I).

differ	ent s	symmetries. (PA)	$K\Gamma(1)$	).										
Prist	ine p	phase(P6/mmm)	SG1	91-P	6/mmm(type I)	SG19	91-P	6/mmm(type II)	SG1	94-P	$6_3/\text{mmc}(\text{type I})$	SG19	4-P6	3/mmc(type II)
	WP	Coordinates		WP			WP	Coordinates		WP	Coordinates		WP	Coordinates
			Ge1		(0, 0, 0)	Ge1		(0, 0, z)	Ge1		(0, 0, 0)	Ge1	2b	(0, 0, 1/4)
Ge1	1a	(0, 0, 0)							1					
		( , , ,	Ge2		(0, 0, 1/2)	Ge2	61	(1/2, 0, z)	Ge2	bg	(1/2, 0, 0)	Ge2	6h	(x, 2x, 1/4)
			Ge3		(1/2, 0, 0)									
			Ge4	3g	(1/2, 0, 1/2)									
$\overline{\text{Ge}2}$	2d	(1/3, 2/3, 1/2)	Ge5		(1/3, 2/3, z)	Ge3	2c	(1/3, 2/3, 0)	Ge3	2c	(1/3, 2/3, 1/4)	Ge3	4f	(1/3, 2/3, z)
~~ <b>_</b>		(1/0, 1/0, 1/1)		12o	(x, 2x, z)	Ge4		(1/3, 2/3, 1/2)	Ge4		(1/3, 2/3, 1/4)	Ge4		(x, 2x, z)
			Geo	120	(x, 2x, z)	l			1			Ge4	12K	$(x, \Delta x, Z)$
						Ge5		(x, 2x, 0)	Ge5		(x, 2x, 1/4)			
						Ge6		(x, 2x, 1/2)	Ge6		(x, 2x, 1/4)			
			Fe1	6j	(x, 0, 0)	Fe1	12n	(x, 2x, z)	Fe1	12k	(x, 0, 0)	Fe1	6h	(x, 2x, 1/4)
Fe	3f	(1/2, 0, 0))	Fe2		(x, 0, 1/2)	Fe2	120	(x, 0, z)	Fe2	12k	(x, 2x, z)	Fe2	6h	(x, 2x, 1/4)
- 0	01	(1/2, 0, 0))	Fe3	6l	(x, 2x, 0)	102		(11, 0, 2)	- 0 -		(11, 211, 2)	Fe3	12j	(x, y, 1/4)
			1									100	1 <i>2</i> J	(x, y, 1/4)
			ге4	6m	(x, 2x, 1/2)									
Prist	ine p	phase(P6/mmm)	SG1	93-P	$6_3/\text{mcm}(\text{type I})$	SG19	93-P	$6_3/\text{mcm}(\text{type II})$	SG	192-F	P6/mcc(type I)	SG1	92-P	6/mcc(type II)
	WP	Coordinates		WP			WP	Coordinates			, (01 )		WP	Coordinates
	***		Ge1		(0, 0, 0)	Ge1		(0, 0, 1/4)	Ge1	2h	(0, 0, 0)	Ge1	2b	(0, 0, 1/4)
Ge1	1a	(0, 0, 0)	1											
			Ge2		(1/2, 0, 0)	Ge2		(x, 0, 1/4)	Ge2		(1/2, 0, 0)	Ge2	6f	(1/2, 0, 1/4)
Ge2	24	(1/3, 2/3, 1/2)	Ge3	4c	(1/3, 2/3, 1/4)	Ge3	4d	(1/3, 2/3, 0)	Ge3	4c	(1/3, 2/3, 1/4)	Ge3	4d	(1/3, 2/3, z)
Gez	2u	(1/3, 2/3, 1/2)	Ge4	12j	(x, y, 1/4)	Ge4	12i	(x, 2x, 0)	Ge4	12k	(x, 2x, 1/4)	Ge4	12l	(x, y, 0)
			Fe1		(x, 0, z)	Fe1	6g	(x, 0, 1/4)	Fe1	12l	(x, y, 0)	Fe1	12j	(x, 0, 1/4)
Fe	3f	(1/2, 0, 0))	1	12k		Fe2			Fe2			Fe2		
ге	91	(1/2, 0, 0))	rez	12K	(x 2x, 0)		6g	(x, 0, 1/4)	rez	121	(x, y, 0)	rez	12K	(x, 2x, 1/4)
						Fe3	12 <u>j</u>	(x, y, 1/4)						
Prist	ine r	phase(P6/mmm)	S	$\overline{G190}$	-P62c(type I)	SC	3190	-P62c(type II)	SC	3189-	$P\overline{6}2m(type\ I)$	SG	189-I	P62m(type II)
	WP	Coordinates		WP			WP	Coordinates		WP	Coordinates		WP	Coordinates
-	***	Coordinates	Ge1		(0, 0, 0)	Ge1		(0, 0, 1/4)	Ge1		(0, 0, 0)	Ge1	2e	(0, 0, z)
			1		. , , ,									
Ge1	1a.	(0, 0, 0)	Ge2	6g	(x, 0, 0)	Ge2	6h	(x, y, 1/4)	Ge2		(0, 0, 1/2)	Ge2	6i	(x, 0, z)
001	100	(0, 0, 0)							Ge3	3f	(x, 0, 0)			
									Ge4	3g	(x, 0, 1/2)			
			Ge3	2c	(1/3, 2/3, 1/4)	Ge3	4f	(1/3, 2/3, z)	Ge5		(1/3, 2/3, z)	Ge3	2c	(1/3, 2/3, 0)
			Ge4		(1/3, 2/3, 3/4)						(x, y, z)	Ge4	2d	(1/3, 2/3, 1/2)
Ge2	2d	(1/3, 2/3, 1/2)	!			Ge4	121	(x, y, z)	Geo	121	(x, y, z)			
			Ge5		(x, y, 1/4)							Ge5	6j	(x, y, 0)
			Ge6		(x, y, 1/4)							Ge6	6k	(x, y, 1/2)
			Fe1	6g	(x, 0, 0)	Fe1	6h	(x, y, 1/4)	Fe1	3f	(x, 0, 0)	Fe1	6i	(x, 0, z)
			Fe2	6g	(x, 0, 0)	Fe2	6h	(x, y, 1/4)	Fe2	3f	(x, 0, 0)	Fe2	6i	(x, 0, z)
					(x, y, z)	Fe3	6h	(x, y, 1/4)	Fe3	3g	(x, 0, 1/2)	Fe3	12l	(x, y, z)
Fe	3f	(1/2, 0, 0))	1.60	121	(x, y, z)			(A, y, 1/4)				1.69	121	(x, y, z)
						ге4	OH	(x, y, 1/4)	Fe4	3g	(x, 0, 1/2)			
									Fe5	6j	(x, y, 0)			
									Fe6	6k	(x, y, 1/2)			
Prict	ine r	phase(P6/mmm)	Si	G188	-P6c2(type I)	SC	1188	-P6c2(type II)	SC	1187	P6m2(type I)	SC	187_1	P6m2(type II)
- 1130	WP	Coordinates	<del>                                     </del>		,		WP	Coordinates	50	WP	Coordinates	50	WP	
	vv P	Coordinates	0.1	WP					Q 1			0.1		
				2a	(0, 0, 0)	Ge1		(1/3, 2/3, 1/4)	Ge1		(0, 0, 0)	Ge1	2h	(1/3, 2/3, z)
$C_{01}$	1.	(0, 0, 0)	Ge2	6j	(x, 2x, 0)	Ge2	6k	(x, y, 1/4)	Ge2		(0, 0, 1/2)	Ge2	6n	(x, 2x, z)
Ge1	та	(0, 0, 0)							Ge3	3j	(x, 2x, 0)			
									Ge4		(x, 2x, 1/2)			
			Ge3	2d	(2/3, 1/3, 1/4)	Co2	2a	(0, 0, 0)	Ge5		(2/3, 1/3, z)	Ge3	1a	(0, 0, 0)
			I					* ' '	1					
			Ge4					(2/3, 1/3, 0)	Ge6		(1/3, 2/3, z)	Ge4	1b	(0, 0, 1/2)
			Ge5		(x, y, 1/4)	Ge5	6j	(x, 2x, 0)	Ge7		(x, 2x, z)	Ge5	1e	(2/3, 1/3, 0)
C-0	0.1	(1/2 9/2 1/9)	Ge6	6k	(x, y, 1/4)	Ge6	6j	(x, 2x, 1/2)	Ge8	6n	(x, 2x, z)	Ge6	1f	(2/3, 1/3, 1/2)
Ge2	2a	(1/3, 2/3, 1/2)			, , , ,							Ge7	3j	(x, 2x, 0)
												Ge8	3j	(x, 2x, 0)
												Ge9	3k	(x, 2x, 1/2)
												Ge10	3k	(x, 2x, 1/2)
			Fe1	6j	(x, 2x, 0)	Fe1	6k	(x, y, 1/4)	Fe1	3j	(x, 2x, 0)	Fe1	6n	(x, 2x, z)
						Fe2	6k	(x, y, 1/4)	Fe2	3j	(x, 2x, 0)	Fe2	6n	(x, 2x, z)
			Fe2	6i	(x, 2x, 0)									
			Fe2 Fe3		(x, 2x, 0) (x, y, z)				1					
Fe	3f	(1/2, 0, 0)			(x, 2x, 0) (x, y, z)	Fe3	6k	(x, y, 1/4)	Fe3	3k	(x, 2x, 1/2)	Fe3	12o	(x, y, z)
Fe	3f	(1/2, 0, 0)				Fe3	6k		Fe3 Fe4	3k 3k	(x, 2x, 1/2) (x, 2x, 1/2)			
Fe	3f	(1/2, 0, 0)				Fe3	6k	(x, y, 1/4)	Fe3 Fe4 Fe5	3k 3k 6l	(x, 2x, 1/2) (x, 2x, 1/2) (x, y, 0)			
Fe	3f	(1/2, 0, 0)				Fe3	6k	(x, y, 1/4)	Fe3 Fe4 Fe5	3k 3k 6l	(x, 2x, 1/2) (x, 2x, 1/2)			

TABLE VII. The corresponding Wyckoff positions and the coordinates of the atoms in the pristine phase and CDW phases with different symmetries. (PART II).

Prist	ine r	phase(P6/mmm)	SG	186-	$P\overline{6}_3$ mc(type I)	SG1	85-P	$\overline{6}_3$ cm(type I)	SG	184-I	P6cc(type I)	SG	183-1	P6mm(type I)
	WP	Coordinates	50	WP	Coordinates	201		Coordinates			Coordinates		WP	Coordinates
			Ge1		(0, 0, z)	Ge1	2a	(0, 0, z)	Ge1	2a	(0, 0, z)	Ge1	1a	(0, 0, z)
C 1	1	(0, 0, 0)	Ge2		$(\mathbf{x}, 0, \mathbf{z})$	Ge2		(x, 2x, z)	Ge2		(1/2, 0, z)	Ge2		(0, 0, z)
Ge1	$^{1a}$	(0, 0, 0)			. , , ,						. , , , ,	Ge3	3c	(1/2, 0, z)
												Ge4	3c	(1/2, 0, z)
			Ge3	4b	(1/3, 2/3, z)	Ge3	2b	(1/3, 2/3, z)	Ge3	4b	(1/3, 2/3, z)	Ge5	2b	(1/3, 2/3, z)
Ge2	2d	(1/3, 2/3, 1/2)	Ge4	12d	(x, y, z)	Ge4		(1/3, 2/3, z)	Ge4	12d	(x, y, z)	Ge6	2b	(1/3, 2/3, z)
GC2	20	(1/3, 2/3, 1/2)				Ge5		(x, 2x, z)				Ge7	6e	(x, 2x, z)
						Ge6		(x, 2x, z)				Ge8	6e	(x, 2x, z)
			Fe1	6c	(x, 0, z)	Fe1	6c	(x, 2x, z)	Fe1		(x, y, z)	Fe1	6d	(x, 0, z)
Fe	3f	(1/2, 0, 0)	Fe2	6c	(x, 0, z)	Fe2	6c	(x, 2x, z)	Fe2	12d	(x, y, z)	Fe2	6d	(x, 0, z)
		( ) , , ,	Fe3	12d	(x, y, z)	Fe3	12d	(x, y, z)				Fe3	6d	(x, 2x, z)
												Fe4	6d	(x, 2x, z)
Prist	ine r	phase(P6/mmm)	SG	1182-	P6 <sub>3</sub> 22(type I)	SG1	82-P	6 <sub>3</sub> 22(type II)	SG	177-I	P622(type I)	SC	177-	P622(type II)
11150	WP	Coordinates		WP	Coordinates	501		Coordinates	50		Coordinates		WP	Coordinates
-	***	Coordinates	Ge1		(0, 0, 0)	Ge1		(0, 0, 1/4)	Ge1	1a	(0, 0, 0)	Ge1		(0, 0, z)
Q 1		(0, 0, 0)	Ge2		(x, 0, 0)	Ge2		(x, 2x, 1/4)	Ge2		(0, 0, 1/2)	Ge2		(1/2, 0, z)
Ge1	$_{1a}$	(0, 0, 0)		O	( , , ,			( , , , , , ,	Ge3	3f	(0, 1/2, 0)			(
									Ge4	3g	(0, 1/2, 1/2)			
			Ge3	2c	(1/3, 2/3, 1/4)	Ge3	4f	(1/3, 2/3, z)	Ge5	4h	(1/3, 2/3, z)	Ge3	2c	(1/3, 2/3, 0)
Ge2	2d	(1/3, 2/3, 1/2)	Ge4		(1/3, 2/3, 3/4)	Ge4	12i	(x, y, z)	Ge6	12n	(x, y, z)	Ge4	2d	(1/3, 2/3, 1/2)
GC2	20	(1/3, 2/3, 1/2)	Ge5	6h	(x, 2x, 1/4)							Ge5		(x, 2x, 0)
			Ge6	6h	(x, 2x, 1/4)							Ge6		(x, 2x, 1/2)
			Fe1	6g	(x, 0, 0)	Fe1	6h	(x, 2x, 1/4)	Fe1	6j	(x, 0, 0)	Fe1		(x, y, z)
Fe	3f	(1/2, 0, 0)	Fe2	6g	(x, 0, 0)	Fe2	6h	(x, 2x, 1/4)	Fe2	6k	(x, 0, 1/2)	Fel	12n	(x, y, z)
		(	Fe3	121	(x, y, z)	Fe3	121	(x, y, z)	Fe3	6l	(x, 2x, 0)			
									Fe4	OIII	(x, 2x, 1/2)			
Prist	ine r	phase(P6/mmm)	SG	176-1	P6 <sub>3</sub> /m(type I)	SG1	76-P	63/m(type II)	SG	175-F	P6/m(type I)	SG	175-1	P6/m(type II)
Prist	ine p	phase(P6/mmm) Coordinates	SG	176-1 WP	P6 <sub>3</sub> /m(type I) Coordinates	SG1		$\frac{6_3/\text{m(type II)}}{\text{Coordinates}}$	SG		26/m(type I) Coordinates	SG		P6/m(type II) Coordinates
Prist		bhase(P6/mmm) Coordinates	Ge1	WP 2b	$\begin{array}{c} P6_3/m(type\ I) \\ \hline Coordinates \\ (0, 0, 0) \end{array}$	SG1 Ge1		$\frac{6_3/\text{m(type II)}}{\text{Coordinates}}$ $\frac{(0, 0, 1/4)}{}$	SG:		$\frac{\text{P6/m(type I)}}{\text{Coordinates}}$ $\frac{(0, 0, 0)}{\text{Coordinates}}$	SG Ge1	175-l WP 2e	P6/m(type II) Coordinates (0, 1/2, z)
	WP	Coordinates		WP 2b	Coordinates		WP 2a	Coordinates		WP 1a 1b	Coordinates		WP 2e	Coordinates
Prist Ge1	WP	. , ,	Ge1	WP 2b	Coordinates $(0, 0, 0)$	Ge1	WP 2a	Coordinates $(0, 0, 1/4)$	Ge1 Ge2 Ge3	WP 1a	Coordinates (0, 0, 0) (0, 0, 1/2) (1/2, 0, 0)	Ge1	WP 2e	Coordinates $(0, 1/2, z)$
	WP	Coordinates	Ge1 Ge2	WP 2b 6g	Coordinates $(0, 0, 0)$ $(1/2, 0, 0)$	Ge1 Ge2	WP 2a 6h	Coordinates (0, 0, 1/4) (x, y, 1/4)	Ge1 Ge2 Ge3 Ge4	WP 1a 1b 3f 3g	Coordinates (0, 0, 0) (0, 0, 1/2) (1/2, 0, 0) (1/2, 0, 1/2)	Ge1 Ge2	WP 2e 6i	Coordinates (0, 1/2, z) (0, 0, z)
	WP	Coordinates	Ge1 Ge2	WP 2b 6g 2c	Coordinates (0, 0, 0) (1/2, 0, 0) (1/3, 2/3, 1/4)	Ge1 Ge2	WP 2a 6h 4f	Coordinates (0, 0, 1/4) (x, y, 1/4) (1/3, 2/3, z)	Ge1 Ge2 Ge3 Ge4 Ge5	WP 1a 1b 3f 3g 4h	Coordinates (0, 0, 0) (0, 0, 1/2) (1/2, 0, 0) (1/2, 0, 1/2) (1/3, 2/3, z)	Ge1 Ge2	WP 2e 6i 2c	Coordinates (0, 1/2, z) (0, 0, z) (1/3, 2/3, 0)
Ge1	WP 1a	Coordinates $(0, 0, 0)$	Ge1 Ge2 Ge3 Ge4	WP 2b 6g 2c 2d	Coordinates (0, 0, 0) (1/2, 0, 0) (1/3, 2/3, 1/4) (1/3, 2/3, 3/4)	Ge1 Ge2	WP 2a 6h 4f	Coordinates (0, 0, 1/4) (x, y, 1/4)	Ge1 Ge2 Ge3 Ge4	WP 1a 1b 3f 3g 4h	Coordinates (0, 0, 0) (0, 0, 1/2) (1/2, 0, 0) (1/2, 0, 1/2)	Ge1 Ge2 Ge3 Ge4	WP 2e 6i 2c 2d	Coordinates (0, 1/2, z) (0, 0, z)  (1/3, 2/3, 0) (1/3, 2/3, 1/2)
Ge1	WP 1a	Coordinates	Ge1 Ge2 Ge3 Ge4 Ge5	WP 2b 6g 2c 2d 6h	Coordinates (0, 0, 0) (1/2, 0, 0) (1/3, 2/3, 1/4) (1/3, 2/3, 3/4) (x, y, 1/4)	Ge1 Ge2	WP 2a 6h 4f	Coordinates (0, 0, 1/4) (x, y, 1/4) (1/3, 2/3, z)	Ge1 Ge2 Ge3 Ge4 Ge5	WP 1a 1b 3f 3g 4h	Coordinates (0, 0, 0) (0, 0, 1/2) (1/2, 0, 0) (1/2, 0, 1/2) (1/3, 2/3, z)	Ge1 Ge2 Ge3 Ge4 Ge5	2c 2d 6j	Coordinates (0, 1/2, z) (0, 0, z)  (1/3, 2/3, 0) (1/3, 2/3, 1/2) (x, y, 0)
Ge1	WP 1a	Coordinates $(0, 0, 0)$	Ge1 Ge2 Ge3 Ge4 Ge5 Ge6	2c 2d 6h 6h	Coordinates (0, 0, 0) (1/2, 0, 0)  (1/3, 2/3, 1/4) (1/3, 2/3, 3/4) (x, y, 1/4) (x, y, 1/4)	Ge1 Ge2 Ge3 Ge4	WP 2a 6h 4f 12i	Coordinates (0, 0, 1/4) (x, y, 1/4)  (1/3, 2/3, z) (x, y, z)	Ge1 Ge2 Ge3 Ge4 Ge5 Ge6	WP 1a 1b 3f 3g 4h 12l	Coordinates (0, 0, 0) (0, 0, 1/2) (1/2, 0, 0) (1/2, 0, 1/2) (1/3, 2/3, z) (x, y, z)	Ge1 Ge2 Ge3 Ge4 Ge5 Ge6	2c 2d 6j 6k	Coordinates $(0, 1/2, z)$ $(0, 0, z)$ $(1/3, 2/3, 0)$ $(1/3, 2/3, 1/2)$ $(x, y, 0)$ $(x, y, 1/2)$
Ge1	WP  1a  2d	Coordinates (0, 0, 0) (1/3, 2/3, 1/2)	Ge1 Ge2 Ge3 Ge4 Ge5 Ge6 Fe1	2c 2d 6h 6h 12i	Coordinates (0, 0, 0) (1/2, 0, 0)  (1/3, 2/3, 1/4) (1/3, 2/3, 3/4) (x, y, 1/4) (x, y, 1/4) (x, y, z)	Ge1 Ge2 Ge3 Ge4	WP 2a 6h 4f 12i 6h	Coordinates (0, 0, 1/4) (x, y, 1/4)  (1/3, 2/3, z) (x, y, z)  (x, y, 1/4)	Ge1 Ge2 Ge3 Ge4 Ge5 Ge6	WP 1a 1b 3f 3g 4h 12l	Coordinates (0, 0, 0) (0, 0, 1/2) (1/2, 0, 0) (1/2, 0, 1/2) (1/3, 2/3, z) (x, y, z)  (x, y, 0)	Ge1 Ge2 Ge3 Ge4 Ge5 Ge6 Fe1	2c 2d 6j 6k 12l	Coordinates (0, 1/2, z) (0, 0, z)  (1/3, 2/3, 0) (1/3, 2/3, 1/2) (x, y, 0) (x, y, 1/2) (x, y, z)
Ge1	WP  1a  2d	Coordinates $(0, 0, 0)$	Ge1 Ge2 Ge3 Ge4 Ge5 Ge6	2c 2d 6h 6h 12i	Coordinates (0, 0, 0) (1/2, 0, 0)  (1/3, 2/3, 1/4) (1/3, 2/3, 3/4) (x, y, 1/4) (x, y, 1/4)	Ge1 Ge2 Ge3 Ge4 Fe1 Fe2	WP 2a 6h 4f 12i 6h 6h	Coordinates (0, 0, 1/4) (x, y, 1/4)  (1/3, 2/3, z) (x, y, z)  (x, y, 1/4) (x, y, 1/4)	Ge1 Ge2 Ge3 Ge4 Ge5 Ge6	WP 1a 1b 3f 3g 4h 12l 6j 6j	Coordinates (0, 0, 0) (0, 0, 1/2) (1/2, 0, 0) (1/2, 0, 1/2) (1/3, 2/3, z) (x, y, z)  (x, y, 0) (x, y, 0)	Ge1 Ge2 Ge3 Ge4 Ge5 Ge6	2c 2d 6j 6k 12l	Coordinates $(0, 1/2, z)$ $(0, 0, z)$ $(1/3, 2/3, 0)$ $(1/3, 2/3, 1/2)$ $(x, y, 0)$ $(x, y, 1/2)$
Ge1	WP  1a  2d	Coordinates (0, 0, 0) (1/3, 2/3, 1/2)	Ge1 Ge2 Ge3 Ge4 Ge5 Ge6 Fe1	2c 2d 6h 6h 12i	Coordinates (0, 0, 0) (1/2, 0, 0)  (1/3, 2/3, 1/4) (1/3, 2/3, 3/4) (x, y, 1/4) (x, y, 1/4) (x, y, z)	Ge1 Ge2 Ge3 Ge4 Fe1 Fe2 Fe3	WP 2a 6h 4f 12i 6h 6h 6h	Coordinates (0, 0, 1/4) (x, y, 1/4)  (1/3, 2/3, z) (x, y, z)  (x, y, 1/4) (x, y, 1/4) (x, y, 1/4)	Ge1 Ge2 Ge3 Ge4 Ge5 Ge6 Fe1 Fe2 Fe3	WP 1a 1b 3f 3g 4h 12l 6j 6k	Coordinates (0, 0, 0) (0, 0, 1/2) (1/2, 0, 0) (1/2, 0, 1/2) (1/3, 2/3, z) (x, y, z)  (x, y, 0) (x, y, 0) (x, y, 1/2)	Ge1 Ge2 Ge3 Ge4 Ge5 Ge6 Fe1	2c 2d 6j 6k 12l	Coordinates (0, 1/2, z) (0, 0, z)  (1/3, 2/3, 0) (1/3, 2/3, 1/2) (x, y, 0) (x, y, 1/2) (x, y, z)
Ge1	WP  1a  2d	Coordinates (0, 0, 0) (1/3, 2/3, 1/2)	Ge1 Ge2 Ge3 Ge4 Ge5 Ge6 Fe1	2c 2d 6h 6h 12i	Coordinates (0, 0, 0) (1/2, 0, 0)  (1/3, 2/3, 1/4) (1/3, 2/3, 3/4) (x, y, 1/4) (x, y, 1/4) (x, y, z)	Ge1 Ge2 Ge3 Ge4 Fe1 Fe2	WP 2a 6h 4f 12i 6h 6h 6h	Coordinates (0, 0, 1/4) (x, y, 1/4)  (1/3, 2/3, z) (x, y, z)  (x, y, 1/4) (x, y, 1/4)	Ge1 Ge2 Ge3 Ge4 Ge5 Ge6	WP 1a 1b 3f 3g 4h 12l 6j 6k	Coordinates (0, 0, 0) (0, 0, 1/2) (1/2, 0, 0) (1/2, 0, 1/2) (1/3, 2/3, z) (x, y, z)  (x, y, 0) (x, y, 0)	Ge1 Ge2 Ge3 Ge4 Ge5 Ge6 Fe1	2c 2d 6j 6k 12l	Coordinates (0, 1/2, z) (0, 0, z)  (1/3, 2/3, 0) (1/3, 2/3, 1/2) (x, y, 0) (x, y, 1/2) (x, y, z)
Ge1 Ge2 Fe	WP  1a  2d  3f	Coordinates (0, 0, 0) (1/3, 2/3, 1/2)	Ge1 Ge2 Ge3 Ge4 Ge5 Ge6 Fe1 Fe2	2c 2d 6h 6h 12i 12i	Coordinates (0, 0, 0) (1/2, 0, 0)  (1/3, 2/3, 1/4) (1/3, 2/3, 3/4) (x, y, 1/4) (x, y, 1/4) (x, y, z)	Ge1 Ge2 Ge3 Ge4 Fe1 Fe2 Fe3 Fe4	4f 12i 6h 6h 6h 6h 6h	Coordinates (0, 0, 1/4) (x, y, 1/4)  (1/3, 2/3, z) (x, y, z)  (x, y, 1/4) (x, y, 1/4) (x, y, 1/4)	Ge1 Ge2 Ge3 Ge4 Ge5 Ge6 Fe1 Fe2 Fe3 Fe4	MP 1a 1b 3f 3g 4h 12l 6j 6j 6k 6k	Coordinates (0, 0, 0) (0, 0, 1/2) (1/2, 0, 0) (1/2, 0, 1/2) (1/3, 2/3, z) (x, y, z)  (x, y, 0) (x, y, 0) (x, y, 1/2)	Ge1 Ge2 Ge3 Ge4 Ge5 Ge6 Fe1 Fe2	2c 2d 6j 6k 12l 12l	Coordinates (0, 1/2, z) (0, 0, z)  (1/3, 2/3, 0) (1/3, 2/3, 1/2) (x, y, 0) (x, y, 1/2) (x, y, z)
Ge1 Ge2 Fe	WP  1a  2d  3f	Coordinates (0, 0, 0) (1/3, 2/3, 1/2) (1/2, 0, 0)	Ge1 Ge2 Ge3 Ge4 Ge5 Ge6 Fe1 Fe2	2c 2d 6h 6h 12i 12i	Coordinates (0, 0, 0) (1/2, 0, 0)  (1/3, 2/3, 1/4) (1/3, 2/3, 3/4) (x, y, 1/4) (x, y, 1/4) (x, y, z) (x, y, z)	Ge1 Ge2 Ge3 Ge4 Fe1 Fe2 Fe3 Fe4	WP 2a 6h 4f 12i 6h 6h 6h 6h 6h 165-H	Coordinates (0, 0, 1/4) (x, y, 1/4)  (1/3, 2/3, z) (x, y, z)  (x, y, 1/4) (x, y, 1/4) (x, y, 1/4) (x, y, 1/4)	Ge1 Ge2 Ge3 Ge4 Ge5 Ge6 Fe1 Fe2 Fe3 Fe4	1a 1b 3f 3g 4h 12l 6j 6k 6k 164-F	Coordinates (0, 0, 0) (0, 0, 1/2) (1/2, 0, 0) (1/2, 0, 1/2) (1/3, 2/3, z) (x, y, z)  (x, y, 0) (x, y, 0) (x, y, 1/2) (x, y, 1/2)	Ge1 Ge2 Ge3 Ge4 Ge5 Ge6 Fe1 Fe2	2c 2d 6j 6k 12l 12l	Coordinates (0, 1/2, z) (0, 0, z)  (1/3, 2/3, 0) (1/3, 2/3, 1/2) (x, y, 0) (x, y, 1/2) (x, y, z) (x, y, z)
Ge1 Ge2 Fe	WP  1a  2d  3f	Coordinates (0, 0, 0) (1/3, 2/3, 1/2) (1/2, 0, 0)  Chase(P6/mmm)	Ge1 Ge2 Ge3 Ge4 Ge5 Ge6 Fe1 Fe2	2c 2d 6h 6h 12i 12i	Coordinates (0, 0, 0) (1/2, 0, 0)  (1/3, 2/3, 1/4) (1/3, 2/3, 3/4) (x, y, 1/4) (x, y, 1/4) (x, y, z) (x, y, z) -P3c1(type I)	Ge1 Ge2 Ge3 Ge4 Fe1 Fe2 Fe3 Fe4	WP 2a 6h 12i 6h 6h 6h 6h WP	Coordinates (0, 0, 1/4) (x, y, 1/4)  (1/3, 2/3, z) (x, y, z)  (x, y, 1/4)	Ge1 Ge2 Ge3 Ge4 Ge5 Ge6 Fe1 Fe2 Fe3 Fe4	1a 1b 3f 3g 4h 12l 6j 6k 6k 164-F	Coordinates (0, 0, 0) (0, 0, 1/2) (1/2, 0, 0) (1/2, 0, 1/2) (1/3, 2/3, z) (x, y, z)  (x, y, 0) (x, y, 0) (x, y, 1/2) (x, y, 1/2)	Ge1 Ge2 Ge3 Ge4 Ge5 Ge6 Fe1 Fe2	2c 2d 6j 6k 12l 12l WP	Coordinates (0, 1/2, z) (0, 0, z)  (1/3, 2/3, 0) (1/3, 2/3, 1/2) (x, y, 0) (x, y, 1/2) (x, y, z) (x, y, z)
Ge1 Ge2 Fe	WP  1a  2d  3f	Coordinates (0, 0, 0) (1/3, 2/3, 1/2) (1/2, 0, 0)  Coordinates	Ge1 Ge2 Ge3 Ge4 Ge5 Ge6 Fe1 Fe2	2c 2d 6h 6h 12i 12i UPP 2b	Coordinates (0, 0, 0) (1/2, 0, 0)  (1/3, 2/3, 1/4) (1/3, 2/3, 3/4) (x, y, 1/4) (x, y, 1/4) (x, y, z) (x, y, z)  (x, y, z)  Coordinates	Ge1 Ge2 Ge3 Ge4 Fe1 Fe2 Fe3 Fe4	4f 12i 6h 6h 6h 6h 6h WP 2a	Coordinates (0, 0, 1/4) (x, y, 1/4)  (1/3, 2/3, z) (x, y, z)  (x, y, 1/4) (x, y, 1/4) (x, y, 1/4) (x, y, 1/4) Coordinates	Ge1 Ge2 Ge3 Ge4 Ge5 Ge6 Fe1 Fe2 Fe3 Fe4	10 10 10 10 10 10 10 10 10 10 10 10 10 1	Coordinates $(0, 0, 0)$ $(0, 0, 1/2)$ $(1/2, 0, 0)$ $(1/2, 0, 1/2)$ $(1/3, 2/3, z)$ $(x, y, z)$ $(x, y, 0)$ $(x, y, 0)$ $(x, y, 1/2)$ $(x, y, 1/2)$ Coordinates	Ge1 Ge2 Ge3 Ge4 Ge5 Ge6 Fe1 Fe2	2c 2d 6j 6k 12l 12l 164-l WP 2c	Coordinates (0, 1/2, z) (0, 0, z)  (1/3, 2/3, 0) (1/3, 2/3, 1/2) (x, y, 0) (x, y, 1/2) (x, y, z) (x, y, z)  P3m1(type II) Coordinates
Ge1 Ge2 Fe	WP  1a  2d  3f	Coordinates (0, 0, 0) (1/3, 2/3, 1/2) (1/2, 0, 0)  Chase(P6/mmm)	Ge1 Ge2 Ge3 Ge4 Ge5 Ge6 Fe1 Fe2	2c 2d 6h 6h 12i 12i UPP 2b	Coordinates (0, 0, 0) (1/2, 0, 0)  (1/3, 2/3, 1/4) (1/3, 2/3, 3/4) (x, y, 1/4) (x, y, 1/4) (x, y, z) (x, y, z)  (x, y, z)  Coordinates (0, 0, 0)	Ge1 Ge2 Ge3 Ge4 Fe1 Fe2 Fe3 Fe4 SG	4f 12i 6h 6h 6h 6h 6h WP 2a	Coordinates (0, 0, 1/4) (x, y, 1/4)  (1/3, 2/3, z) (x, y, z)  (x, y, 1/4) (x, y, 1/4) (x, y, 1/4) (x, y, 1/4)  Coordinates (0, 0, 1/4)	Ge1 Ge2 Ge3 Ge4 Ge5 Ge6 Fe1 SG: Ge1 Ge2 Ge3	WP   1a   1b   3f   3g   4h   12l     6j   6k   6k     U64-F   WP   1a   1b   3e	Coordinates (0, 0, 0) (0, 0, 1/2) (1/2, 0, 0) (1/2, 0, 1/2) (1/3, 2/3, z) (x, y, z)  (x, y, 0) (x, y, 1/2) (x, y, 1/2)  Coordinates (0, 0, 0) (0, 0, 1/2) (0, 1/2, 0)	Ge1 Ge2 Ge3 Ge4 Ge5 Ge6 Fe1 Fe2	2c 2d 6j 6k 12l 12l 164-l WP 2c	Coordinates (0, 1/2, z) (0, 0, z)  (1/3, 2/3, 0) (1/3, 2/3, 1/2) (x, y, 0) (x, y, 1/2) (x, y, z) (x, y, z) (x, y, z)  Pam1(type II) Coordinates (0, 0, z)
Ge1 Ge2 Fe	WP  1a  2d  3f	Coordinates (0, 0, 0) (1/3, 2/3, 1/2) (1/2, 0, 0)  Coordinates	Ge1 Ge2 Ge3 Ge4 Ge5 Ge6 Fe1 Fe2	2c 2d 6h 6h 12i 12i WP 2b 6e	Coordinates $(0, 0, 0)$ $(1/2, 0, 0)$ $(1/3, 2/3, 1/4)$ $(1/3, 2/3, 3/4)$ $(x, y, 1/4)$ $(x, y, 1/4)$ $(x, y, z)$	Ge1 Ge2 Ge3 Ge4 Fe1 Fe2 Fe3 Fe4 SG	## WP 2a 6h 6h 6h 6h 6h WP 2a 6f	Coordinates (0, 0, 1/4) (x, y, 1/4)  (1/3, 2/3, z) (x, y, z)  (x, y, 1/4) (x, y, 1/4) (x, y, 1/4) (x, y, 1/4)  Coordinates (0, 0, 1/4) (x, 0, 1/4)	Ge1 Ge2 Ge3 Ge4 Ge5 Ge6 Fe1 Ge1 Ge2 Ge3 Ge4	WP   1a   1b   3f   3g   4h   12l     6j   6k   6k     WP   1a   1b   3e   3f	(0, 0, 0) (0, 0, 1/2) (1/2, 0, 0) (1/2, 0, 1/2) (1/3, 2/3, z) (x, y, z) (x, y, 0) (x, y, 1/2) (x, y, 1/2)	Ge1 Ge2 Ge3 Ge4 Ge5 Ge6 Fe1 Fe2	2c 2d 6j 6k 12l 12l WP 2c 6i	Coordinates (0, 1/2, z) (0, 0, z)  (1/3, 2/3, 0) (1/3, 2/3, 1/2) (x, y, 0) (x, y, 1/2) (x, y, z) (x, y, z)  P3m1(type II) Coordinates (0, 0, z) (x, 2x z)
Ge1 Ge2 Fe	WP  1a  2d  3f	Coordinates (0, 0, 0) (1/3, 2/3, 1/2) (1/2, 0, 0)  Coordinates	Ge1 Ge2 Ge3 Ge4 Ge5 Ge6 Fe1 Fe2	2c 2d 6h 6h 12i 12i WP 2b 6e 4d	Coordinates (0, 0, 0) (1/2, 0, 0)  (1/3, 2/3, 1/4) (1/3, 2/3, 3/4) (x, y, 1/4) (x, y, 1/4) (x, y, z) (x, y, z)  -P3c1(type I)  Coordinates (0, 0, 0) (1/2, 0, 0)  (1/3, 2/3, z)	Ge1 Ge2 Ge3 Ge4 Fe1 Fe2 Fe3 Fe4 SG Ge1 Ge2	WP 2a 6h 12i 6h 6h 6h 6h 6h 4d 6f 6f 4d	Coordinates (0, 0, 1/4) (x, y, 1/4)  (1/3, 2/3, z) (x, y, z)  (x, y, 1/4) (x, y, 1/4) (x, y, 1/4) (x, y, 1/4)  Coordinates (0, 0, 1/4) (x, 0, 1/4) (1/3, 2/3, z)	Ge1 Ge2 Ge3 Ge4 Ge5 Ge6 Fe1 Ge1 Ge2 Ge3 Ge4 Ge5	WP   1a   1b   3f   3g   4h   12l     6j   6k   6k     WP   1a   1b   3e   3f   2d	(0, 0, 0) (0, 0, 1/2) (1/2, 0, 0) (1/2, 0, 1/2) (1/3, 2/3, z) (x, y, 0) (x, y, 0) (x, y, 1/2) (x, y, 1/2)	Ge1 Ge2 Ge3 Ge4 Ge5 Ge6 Fe1 Fe2 SG	2c 2d 6j 6k 12l 12l WP 2c 6i	Coordinates (0, 1/2, z) (0, 0, z)  (1/3, 2/3, 0) (1/3, 2/3, 1/2) (x, y, 0) (x, y, 1/2) (x, y, z) (x, y, z) (x, y, z)  P3m1(type II) Coordinates (0, 0, z) (x, 2x z)
Ge1  Fe  Prist	WP  1a  2d  3f  WP  1a	Coordinates (0, 0, 0) (1/3, 2/3, 1/2) (1/2, 0, 0)  Coordinates (0, 0, 0)	Ge1 Ge2 Ge3 Ge4 Ge5 Ge6 Fe1 Fe2	2c 2d 6h 6h 12i 12i WP 2b 6e 4d	Coordinates $(0, 0, 0)$ $(1/2, 0, 0)$ $(1/3, 2/3, 1/4)$ $(1/3, 2/3, 3/4)$ $(x, y, 1/4)$ $(x, y, 1/4)$ $(x, y, z)$	Ge1 Ge2 Ge3 Ge4 Fe1 Fe2 Fe3 Fe4 SG Ge1 Ge2	## WP 2a 6h 6h 6h 6h 6h WP 2a 6f	Coordinates (0, 0, 1/4) (x, y, 1/4)  (1/3, 2/3, z) (x, y, z)  (x, y, 1/4) (x, y, 1/4) (x, y, 1/4) (x, y, 1/4)  Coordinates (0, 0, 1/4) (x, 0, 1/4)	Ge1 Ge2 Ge3 Ge4 Ge5 Ge6 Fe1 Ge1 Ge2 Ge3 Ge4 Ge5 Ge6	WP   1a   1b   3f   3g   4h   12l     6j   6k   6k     WP   1a   1b   3e   3f   2d   2d   2d	Coordinates (0, 0, 0) (0, 0, 1/2) (1/2, 0, 0) (1/2, 0, 1/2) (1/3, 2/3, z) (x, y, z)  (x, y, 0) (x, y, 1/2) (x, y, 1/2)  Coordinates (0, 0, 0) (0, 0, 1/2, 0) (0, 1/2, 0) (1/3, 2/3, z) (1/3, 2/3, z)	Ge1 Ge2 Ge3 Ge4 Ge6 Fe1 Fe2 Ge1 Ge2	2c 2d 6j 6k 12l 12l WP 2c 6i 2d	Coordinates (0, 1/2, z) (0, 0, z)  (1/3, 2/3, 0) (1/3, 2/3, 1/2) (x, y, 0) (x, y, 1/2) (x, y, z) (x, y, z) (x, y, z)  P3m1(type II) Coordinates (0, 0, z) (x, 2x z)  (1/3, 2/3, z) (1/3, 2/3, z)
Ge1  Fe  Prist	WP  1a  2d  3f  WP  1a	Coordinates (0, 0, 0) (1/3, 2/3, 1/2) (1/2, 0, 0)  Coordinates	Ge1 Ge2 Ge3 Ge4 Ge5 Ge6 Fe1 Fe2	2c 2d 6h 6h 12i 12i WP 2b 6e 4d	Coordinates (0, 0, 0) (1/2, 0, 0)  (1/3, 2/3, 1/4) (1/3, 2/3, 3/4) (x, y, 1/4) (x, y, 1/4) (x, y, z) (x, y, z)  -P3c1(type I)  Coordinates (0, 0, 0) (1/2, 0, 0)  (1/3, 2/3, z)	Ge1 Ge2 Ge3 Ge4 Fe1 Fe2 Fe3 Fe4 SG Ge1 Ge2	WP 2a 6h 12i 6h 6h 6h 6h 6h 4d 6f 6f 4d	Coordinates (0, 0, 1/4) (x, y, 1/4)  (1/3, 2/3, z) (x, y, z)  (x, y, 1/4) (x, y, 1/4) (x, y, 1/4) (x, y, 1/4)  Coordinates (0, 0, 1/4) (x, 0, 1/4) (1/3, 2/3, z)	Ge1 Ge2 Ge3 Ge4 Ge5 Fe3 Fe4 SG: Ge1 Ge2 Ge3 Ge4 Ge5 Ge6 Ge6	WP   1a   1b   3f   3g   4h   12l     6j   6k   6k     WP   1a   1b   3e   3f   2d   2d   6i	(x, y, 0) (x, y, 1/2) (x, y, y, 1/2) (x, y, y, 1/2) (x, y,	Ge1 Ge2 Ge3 Ge4 Ge6 Fe1 Fe2 Ge1 Ge2 Ge3 Ge4 Ge5	2c 2d 6j 6k 12l 12l WP 2c 6i 2d 2d 6i 6i	Coordinates (0, 1/2, z) (0, 0, z)  (1/3, 2/3, 0) (1/3, 2/3, 1/2) (x, y, 0) (x, y, 1/2) (x, y, z) (x, y, z)  P3m1(type II) Coordinates (0, 0, z) (x, 2x z)  (1/3, 2/3, z) (1/3, 2/3, z) (x, 2x, z)
Ge1  Fe  Prist	WP  1a  2d  3f  WP  1a	Coordinates (0, 0, 0) (1/3, 2/3, 1/2) (1/2, 0, 0)  Coordinates (0, 0, 0)	Ge1 Ge2 Ge3 Ge4 Ge5 Ge6 Fe1 Fe2 SC Ge1 Ge2	2c 2d 6h 6h 12i 12i WP 2b 6e 4d 12g	Coordinates (0, 0, 0) (1/2, 0, 0)  (1/3, 2/3, 1/4) (1/3, 2/3, 3/4) (x, y, 1/4) (x, y, 1/4) (x, y, z) (x, y, z)  -P3c1(type I)  Coordinates (0, 0, 0) (1/2, 0, 0)  (1/3, 2/3, z) (x, y, z)	Ge1 Ge2 Ge3 Ge4 Fe1 Fe2 Fe3 Fe4 Ge1 Ge2 Ge3 Ge4	WP 2a 6h 12i 6h 6h 6h 165-H WP 2a 6f 4d 12g	Coordinates (0, 0, 1/4) (x, y, 1/4)  (1/3, 2/3, z) (x, y, z)  (x, y, 1/4) (x, y, 1/4) (x, y, 1/4) (x, y, 1/4) Coordinates (0, 0, 1/4) (x, 0, 1/4) (x, 0, 1/4)	Ge1 Ge2 Ge3 Ge4 Ge5 Fe3 Fe4 SG2 Ge1 Ge2 Ge3 Ge4 Ge5 Ge6 Ge7 Ge8	WP   1a   1b   3f   3g   4h   12l     6j   6k   6k     1b   3e   3f   2d   6i   6i   6i	Coordinates (0, 0, 0) (0, 0, 1/2) (1/2, 0, 0) (1/2, 0, 1/2) (1/3, 2/3, z) (x, y, z)  (x, y, 0) (x, y, 1/2) (x, y, 1/2)  Coordinates (0, 0, 0) (0, 0, 1/2, 0) (0, 1/2, 0) (1/3, 2/3, z) (1/3, 2/3, z) (x, 2x, z) (x, 2x, z) (x, 2x, z)	Ge3 Ge4 Ge5 Ge6 Fe1 Fe2 Ge3 Ge4 Ge5 Ge6	2c 2d 6j 6k 12l 12l WP 2c 6i 6i 6i 6i 6i	Coordinates (0, 1/2, z) (0, 0, z)  (1/3, 2/3, 0) (1/3, 2/3, 1/2) (x, y, 0) (x, y, 1/2) (x, y, z) (x, y, z) (x, y, z)  P3m1(type II) Coordinates (0, 0, z) (x, 2x z)  (1/3, 2/3, z) (1/3, 2/3, z) (x, 2x, z) (x, 2x, z)
Ge1  Fe  Prist  Ge1  Ge2	WP  1a  2d  3f  ine p WP  1a  2d	Coordinates (0, 0, 0) (1/3, 2/3, 1/2) (1/2, 0, 0) Chase(P6/mmm) Coordinates (0, 0, 0) (1/3, 2/3, 1/2)	Ge1 Ge2 Ge3 Ge4 Ge5 Ge6 Fe1 Fe2 Ge1 Ge2 Ge3 Ge4	2c 2d 6h 6h 12i 12i WP 2b 6e 4d 12g 12g	Coordinates (0, 0, 0) (1/2, 0, 0)  (1/3, 2/3, 1/4) (1/3, 2/3, 3/4) (x, y, 1/4) (x, y, 1/4) (x, y, z) (x, y, z)  -P3c1(type I)  Coordinates (0, 0, 0) (1/2, 0, 0)  (1/3, 2/3, z) (x, y, z)  (x, y, z)	Ge1 Ge2 Ge3 Ge4 Fe1 SG Ge1 Ge2 Ge3 Ge4	WP 2a 6h 12i 6h 6h 6h 6h 165-F WP 2a 6f 6f 6f	Coordinates (0, 0, 1/4) (x, y, 1/4)  (1/3, 2/3, z) (x, y, z)  (x, y, 1/4) (x, y, 1/4) (x, y, 1/4) (x, y, 1/4)  Coordinates (0, 0, 1/4) (x, 0, 1/4) (x, y, z)	Ge1 Ge2 Ge3 Ge4 Ge5 Fe3 Fe4 SG: Ge1 Ge2 Ge3 Ge4 Ge5 Ge6 Ge7 Ge8	NP   1a   1b   3f   3g   4h   12l   6j   6k   6k   1b   3e   3f   2d   2d   6i   6i   6i   6i	Coordinates $(0, 0, 0)$ $(0, 0, 1/2)$ $(1/2, 0, 0)$ $(1/2, 0, 1/2)$ $(1/3, 2/3, z)$ $(x, y, z)$ $(x, y, 0)$ $(x, y, 1/2)$ $(x, y, 1/2)$ $(x, y, 1/2)$ Coordinates $(0, 0, 0)$ $(0, 0, 1/2)$ $(0, 1/2, 0)$ $(0, 1/2, 1/2)$ $(1/3, 2/3, z)$ $(x, 2x, z)$ $(x, 2x, z)$ $(x, 2x, z)$	Ge3 Ge4 Ge5 Ge6 Fe1 Ge3 Ge4 Ge5 Ge6 Fe1	2c 2d 6j 6k 12l 12l WP 2c 6i 6i 6i 6i 6i 6i	Coordinates $(0, 1/2, z)$ $(0, 0, z)$ $(1/3, 2/3, 0)$ $(1/3, 2/3, 1/2)$ $(x, y, 0)$ $(x, y, 1/2)$ $(x, y, z)$
Ge1  Fe  Prist	WP  1a  2d  3f  WP  1a	Coordinates (0, 0, 0) (1/3, 2/3, 1/2) (1/2, 0, 0)  Coordinates (0, 0, 0)	Ge1 Ge2 Ge3 Ge4 Ge5 Ge6 Fe1 Fe2 Ge1 Ge2 Ge3 Ge4	2c 2d 6h 6h 12i 12i WP 2b 6e 4d 12g	Coordinates (0, 0, 0) (1/2, 0, 0)  (1/3, 2/3, 1/4) (1/3, 2/3, 3/4) (x, y, 1/4) (x, y, 1/4) (x, y, z) (x, y, z)  -P3c1(type I)  Coordinates (0, 0, 0) (1/2, 0, 0)  (1/3, 2/3, z) (x, y, z)	Ge1 Ge2 Fe1 Fe2 Fe3 Fe4 Ge1 Ge2 Ge3 Ge4	WP 2a 6h 12i 6h 6h 6h 165-H WP 2a 6f 4d 12g	Coordinates (0, 0, 1/4) (x, y, 1/4)  (1/3, 2/3, z) (x, y, z)  (x, y, 1/4) (x, y, 1/4) (x, y, 1/4) (x, y, 1/4) Coordinates (0, 0, 1/4) (x, 0, 1/4) (x, 0, 1/4)	Ge1 Ge2 Ge3 Ge4 Ge5 Fe3 Fe4 SG2 Ge1 Ge2 Ge3 Ge4 Ge5 Ge6 Ge7 Ge8	WP   1a   1b   3f   3g   4h   12l   6j   6k   6k   WP   1a   1b   3e   3f   2d   6i   6i   6i   6i   6i   6i   6i   6	Coordinates (0, 0, 0) (0, 0, 1/2) (1/2, 0, 0) (1/2, 0, 1/2) (1/3, 2/3, z) (x, y, z)  (x, y, 0) (x, y, 1/2) (x, y, 1/2)  Coordinates (0, 0, 0) (0, 0, 1/2, 0) (0, 1/2, 0) (1/3, 2/3, z) (1/3, 2/3, z) (x, 2x, z) (x, 2x, z) (x, 2x, z)	Ge3 Ge4 Ge5 Ge6 Fe1 Fe2 Ge3 Ge4 Ge5 Ge6	2c 2d 6j 6k 12l 12l WP 2c 6i 6i 6i 6i 6i 6i 6i	Coordinates (0, 1/2, z) (0, 0, z)  (1/3, 2/3, 0) (1/3, 2/3, 1/2) (x, y, 0) (x, y, 1/2) (x, y, z) (x, y, z) (x, y, z)  P3m1(type II) Coordinates (0, 0, z) (x, 2x z)  (1/3, 2/3, z) (1/3, 2/3, z) (x, 2x, z) (x, 2x, z)

TABLE VIII. The corresponding Wyckoff positions and the coordinates of the atoms in the pristine phase and CDW phases with different symmetries. (PART III).

Driet	inor	hase(P6/mmm)	\ C(	7169	$\overline{P31c(type\ I)}$	97	1169	P31c(type II)	50	1160	P31m(type I)	SC.	169 I	P31m(type II)
Frist	WP	Coordinates	100	л105- WP		20	WP	,	50	WP		36	WP	Coordinates
	WP	Coordinates	O 1		Coordinates	O 1		Coordinates	0.1		Coordinates	O 1		
			Ge1	2b	(0, 0, 0)	Ge1	2a	(0, 0, 1/4)	Ge1	1a	(0, 0, 0)	Ge1	2e	(0, 0, z)
Ge1	1a	(0, 0, 0)	Ge2	6g	(0, 1/2, 0)	Ge2	6h	(x, 2x, 1/4)	Ge2	1b	(0, 0, 1/2)	Ge2	6k	(x, 0, z)
		(-, -, -,							Ge3	3f	(1/2, 0, 0)			
									Ge4	3g	(1/2, 0, 1/2)			
			Ge3	2c	(1/3, 2/3, 1/4)	Ge3	4f	(1/3, 2/3, z)	Ge5	4h	(1/3, 2/3, z)	Ge3	2c	(1/3, 2/3, 0)
Co2	24	(1/3, 2/3, 1/2)	Ge4	2d	(1/3, 2/3, 3/4)	Ge4	12i	(x, y, z)	Ge6	12l	(x, y, z)	Ge4	2d	(1/3, 2/3, 1/2)
Gez	zu	(1/3, 2/3, 1/2)	Ge5	6h	(x, 2x, 1/4)							Ge5	6i	(x, 2x, 0)
			Ge6	6h	(x, 2x, 1/4)							Ge6	6j	(x, 2x, 1/2)
			Fe1	12i	(x, y, z)	Fe1	6h	(x, 2x, 1/4)	Fe1	6i	(x, 2x, 0)	Fe1	6k	(x, 0, z)
ъ.	o.c	(1 (0 0 0))	Fe2	12i	(x, y, z)	Fe2	6h	(x, 2x, 1/4)	Fe2	6j	(x, 2x, 1/2)	Fe2	6k	(x, 0, z)
Fe	3f	(1/2, 0, 0))				Fe3	12i	(x, y, z)	Fe3	6k	(x, 0, z)	Fe3	12i	(x, y, z)
								( , , , ,	Fe4	6k	(x, 0, z)			( , , , ,
Prist	ine p	phase(P6/mmm)	S	G68-	Ccce(type I)	S	G68-0	Ccce(type II)	SC	368-0	Ccce(type III)	SC	368-C	Ccce(type IV)
	WP	Coordinates		WP	Coordinates		WP	Coordinates		WP	Coordinates		WP	Coordinates
			Ge1	8c	(1/4, 1/4, 0)	Ge1	8e	(x, 1/4, 1/4)	Ge1	8g	(0, 1/4, z)	Ge1	4a	(0, 1/4, 1/4)
Ge1	1a	(0, 0, 0)	Ge2	8d	(0, 0, 0)	Ge2		(0, y, 1/4)	Ge2		(1/4, 0, z)	Ge2	4b	(0, 1/4, 3/4)
					( , , ,			( , 0 , , ,			. , , , ,	Ge3	8h	(1/4, 0, z)
Ge2	2d	(1/3, 2/3, 1/2)	Ge3	8f	(0, y, 1/4)	Ge3	16i	(x, y, z)	Ge3	8f	(0, y, 1/4)	Ge3	16i	(x, y, z)
		(	Ge4	8f	(0, y, 1/4)	Ge4		(x, y, z)	Ge4	8f	(0, y, 1/4)	Ge4		(x, y, z)
			Ge5		(x, y, z)			( , 0 , )	Ge5		(x, y, z)			( / 0 / )
			Fe1	8g	(0, 1/4, z)	Fe1	4a	(0, 1/4, 1/4)	Fe1	8c	(1/4, 1/4, 0)	Fe1	8e	(x, 1/4, 1/4)
			Fe2	8h	(1/4, 0, z)	Fe2	4b	(0, 1/4, 3/4)	Fe2	8d	(0, 0, 1/2)	Fe2	8f	(0, y, 1/4)
Fe	3f	(1/2, 0, 0))	Fe3	16i	(x, y, z)	Fe3	8h	(1/4, 0, z)	Fe3	16i	(x, y, z)	Fe3	16i	(x, y, z)
		(	Fe4		(x, y, z)	Fe4	16i	(x, y, z)	Fe4		(x, y, z)	Fe4		(x, y, z)
					( , 0 , )	Fe5		(x, y, z)			( , 0 , )			( / 0 / )
								( , 0 , )						
Prist	ine p	phase(P6/mmm)	SC	367-C	Cmme(type I)	SC	67-C	mme(type II)	SG	67-C	mme(type III)	SG	67-C1	mme(type IV)
	WP	Coordinates		WP	Coordinates		WP	Coordinates		WP	Coordinates		WP	Coordinates
			Ge1	4c	(0, 0, 0)	Ge1		(1/4, 0, 0)	Ge1	4g	(0, 1/4, z)	Ge1	8n	(x, 1/4, z)
O 1		(0, 0, 0)	Ge2		(0, 0, 1/2)	l	4b	(1/4, 0, 1/2)	Ge2	4g	(0, 1/4, z)	Ge2		(0, y, z)
Ge1	$_{1a}$	(0, 0, 0)	Ge3	4e	(1/4, 1/4, 0)	Ge3	4g	(0, 1/4, z)	Ge3	8l	(1/4, 0, z)			( ) 0 / )
			Ge4	4f	(1/4, 1/4, 1/2)	Ge4	4g	(0, 1/4, z)			(			
			Ge5		(0, y, z)	Ge5		(0, y, z)	Ge4	8j	(1/4, y, 0)	Ge3	8j	(1/4, y, 0)
~ ~		(4 (0 0 (0 4 (0)	Ge6		(0, y, z)	Ge6		(0, y, z)	Ge5		(1/4, y, 1/2)	Ge4		(1/4, y, 1/2)
Ge2	2d	(1/3, 2/3, 1/2)	Ge7		(x, y, z)	Ge7		(x, y, z)	Ge6		(0, y, z)	Ge5		(0, y, z)
					( , 0 , )			( , 0 , ,	Ge7		(0, y, z)	Ge6		(0, y, z)
			Fe1	4a	(1/4, 0, 0)	Fe1	4c	(0, 0, 0)	Fe1	8n	(x, 1/4, z)	Fe1	4g	(0, 1/4, z)
			Fe2	4b	(1/4, 0, 1/2)	Fe2	4d	(0, 0, 1/2)	Fe2	8m	(0, y, z)	Fe2	4g	(0, 1/4, z)
Б	o.c	(1 (0 0 0))	Fe3	4g	(0, 1/4, z)	Fe3	4e	(1/4, 1/4, 0)	Fe3	16o	(x, y, z)	Fe3	8 <u>l</u>	(1/4, 0, z)
Fe	31	(1/2, 0, 0))	Fe4		(0, 1/4, z)		4f	(1/4, 1/4, 1/2)			(x, y, z)	Fe4		(x, y, z)
				16o	(x, y, z)		16o	(x, y, z)			( , 0 , ,	Fe5		(x, y, z)
			Fe6		(x, y, z)		16o	(x, y, z)						( , 0 , ,
						ı								
Prist		phase(P6/mmm)	S		Cccm(type I)	SC	366-C	Cccm(type II)	SG		ccm(type III)	SG		ccm(type IV)
	WP	Coordinates		WP	Coordinates		WP	Coordinates		WP	Coordinates		WP	Coordinates
	•		Ge1	4c	(0, 0, 0)	Ge1	4a	(0, 0, 1/4)	Ge1	8l	(x, y, 0)	Ge1		(x, 0, 1/4)
Ge1	1.0	(0, 0, 0)	Ge2	4d	(0, 0, 1/2)	Ge2	4b	(0, 1/2, 1/4)	Ge2	81	(x, y, 0)	Ge2	8h	(0, y, 1/4)
Gei	1a	(0, 0, 0)	Ge3	4e	(1/4, 1/4, 0)	Ge3	8k	(1/4, 1/4, 1/4)						
			Ge4	4f	(1/4, 1/4, 1/2)									
			Ge5	8h	(0, y, 1/4)	Ge4	81	(x, y, 0)	Ge3	8h	(0, y, 1/4)	Ge3	81	(x, y, 0)
Co2	24	(1/3, 2/3, 1/2)	Ge6		(0, y, 1/4)	Ge5	81	(x, y, 0)	Ge4	8h	(0, y, 1/4)	Ge4	81	(x, y, 0)
Gez	zu	(1/3, 2/3, 1/2)	Ge7	16m	(x, y, z)	Ge6		(x, y, 0)	Ge5	16m	(x, y, z)	Ge5	81	(x, y, 0)
						Ge7		(x, y, 0)				Ge6		(x, y, 0)
			Fe1	8l	(x, y, 0)	Fe1		(x, 0, 1/4)	Fe1	4c	(0, 0, 0)	Fe1		(0, 0, 1/4)
			Fe2	8l	(x, y, 0)	Fe2		(0, y, 1/4)	Fe2	4d	(0, 0, 1/2)	Fe2		(0, 1/2, 1/4)
			Fe3	8l	(x, y, 0)	Fe3	$16 \mathrm{m}$	(x, y, z)	Fe3	4e	(1/4, 1/4, 0)	Fe3	8k	(1/4, 1/4, 1/4)
177-	or	(1/9 0 0))	Fe4	8l	(x, y, 0)	Fe4	16m	(x, y, z)	Fe4	4f	(1/4, 1/4, 1/2)	Fe4		(x, y, z)
Fe	3f	(1/2, 0, 0))	Fe5	8l	(x, y, 0)			,	Fe5	8l	(x, y, 0)		$16 \mathrm{m}$	(x, y, z)
			Fe6	8l	(x, y, 0)				Fe6	8l	(x, y, 0)			
									Fe7	8l	(x, y, 0)			
									Fe8	8l	(x, y, 0)			
		<del></del>												

TABLE IX. The corresponding Wyckoff positions and the coordinates of the atoms in the pristine phase and CDW phases with different symmetries.  $(PART\ IV)$ .

		$\frac{\text{Share}(P6/\text{mmm})}{\text{Share}(P6/\text{mmm})}$		,	mmm(type I)	80	165 C	mmm(case2)	SCE	5 Cm	mm(type III)	SCE	. Cm	mm(tring IV)
Prist	WP		56	WP		50	WP		560		Coordinates			Coordinates
	WF	Coordinates	O 1		Coordinates	O 1		Coordinates	O 1					
			Ge1		(0, 0, 0)	Ge1	4i	(0, y, 0)	Ge1		(0, 0, z)	Ge1		(x, 0, z)
			Ge2		(0, 1/2, 0)	Ge2	$_{4j}$	(0, y, 1/2)	Ge2		(0, 1/2, z)	Ge2	8n	(0, y, z)
Ge1	1a	(0, 0, 0)	Ge3		(0, 1/2, 1/2)	Ge3	4g	(x, 0, 0)	Ge3	8m	(1/4, 1/4, z)			
		(	Ge4		(0, 0, 1/2)	Ge4	4h	(x, 0, 1/2)						
			Ge5		(1/4, 1/4, 0)									
			Ge6		(1/4, 1/4, 1/2)			(0)	~ .		(2 2)	~ ~		(0
			Ge7		(0, y, z)	Ge5	8n	(0, y, z)	Ge4		(0, y, 0)	Ge3	4i	(0, y, 0)
			Ge8		(0, y, z)	Ge6	8n	(0, y, z)	Ge5		(0, y, 0)	Ge4	4i	(0, y, 0)
Ge2	2d	(1/3, 2/3, 1/2)	Ge9	16r	(x, y, z)	Ge7	16r	(x, y, z)	Ge6	4j	(0, y, 1/2)	Ge5	4j	(0, y, 1/2)
		(-/ =, -/ =, -/ -)							Ge7	$^{4j}$	(0, y, 1/2)	Ge6	$_{\rm 4j}$	(0, y, 1/2)
									Ge8	-	(x, y, 0)	Ge7	8p	(x, y, 0)
									Ge9	8q	(x, y, 1/2)	Ge8	8q	(x, y, 1/2)
			Fe1	4g	(x, 0, 0)	Fe1	2a	(0, 0, 0)	Fe1	80	(x, 0, z)	Fe1	4k	(0, 0, z)
			Fe2	4h	(x, 0, 1/2)	Fe2	$^{2b}$	(0, 1/2, 0)	Fe2		(0, y, z)	Fe2	41	(0, 1/2, z)
			Fe3	4i	(0, y, 0)	Fe3	2c	(0, 1/2, 1/2)	Fe3		(x, y, z)	Fe3	8m	(1/4, 1/4, z)
			Fe4	4j	(0, y, 1/2)	Fe4	2d	(0, 0, 1/2)	Fe4	16r	(x, y, z)	Fe4		(x, y, z)
Fe	3f	(1/2, 0, 0)	Fe5	8p	(x, y, 0)	Fe5	4e	(1/4, 1/4, 0)				Fe5	16r	(x, y, z)
1.6	91	(1/2, 0, 0)	Fe6	8p	(x, y, 0)	Fe6	4f	(1/4, 1/4, 1/2)						
			Fe7	8q	(x, y, 1/2)	Fe7	8p	(x, y, 0)						
			Fe8	8q	(x, y, 1/2)	Fe8	8p	(x, y, 0)						
						Fe9	8q	(x, y, 1/2)						
						Fe10	8q	(x, y, 1/2)						
			•											
Prist		phase(P6/mmm)	S		Cmce(type I)	SC	364-C	mce(type II)	SG6		nce(type III)			nce(type IV)
	WP	Coordinates		WP	Coordinates		WP	Coordinates			Coordinates			Coordinates
			Ge1	4a	(0, 0, 0)	Ge1	4a	(0, 0, 0)	Ge1	8e	(1/4, y, 1/4)	Ge1	8e	(1/4, y, 1/4)
Ge1	1a	(0, 0, 0)	Ge2	4b	(0, 0, 1/2)	Ge2	4b	(0, 0, 1/2)	Ge2	8f	(0, y, z)	Ge2	8f	(0, y, z)
			Ge3	8c	(1/4, 1/4, 0)	Ge3	8c	(1/4, 1/4, 0)						
			Ge4	16g	(x, y, z)	Ge4	8e	(1/4, y, 1/4)	Ge3	8d	(x, 0, 0)	Ge3	8f	(0, y, z)
Co2	24	(1/3, 2/3, 1/2)	Ge5	16g	(x, y, z)	Ge5	8e	(1/4, y, 1/4)	Ge4	8d	(x, 0, 0)	Ge4	8f	(0, y, z)
Gez	2u	(1/3, 2/3, 1/2)				Ge6	8f	(0, y, z)	Ge5	16g	(x, y, z)	Ge5	16g	(x, y, z)
						Ge7	8f	(0, y, z)						
			Fe1	8d	(x, 0, 0)	Fe1	8e	(1/4, y, 1/4)	Fe1	8e	(1/4, y, 1/4)	Fe1	8e	(1/4, y, 1/4)
			Fe2	8f	(0, y, z)	Fe2	8f	(0, y, z)	Fe2		(0, y, z)	Fe2	8f	(0, y, z)
Fe	3f	(1/2, 0, 0))	Fe3	16g	(x, y, z)	Fe3	16g	(x, y, z)	Fe3	16g	(x, y, z)	Fe3	16g	(x, y, z)
		(	Fe4	_	(x, y, z)	Fe4	_	(x, y, z)	Fe4	_	(x, y, z)	Fe4	_	(x, y, z)
					( , 0 , )		Ü	( , 0 , )		Ü	( , 0 , )			( , 0 , )
-			1			1			1			1		
Prist	ine p	hase(P6/mmm)	SC	364-C	Cmce(type V)	SG	64-C	mce(type VI)	SG6	64-Cn	nce(type VII)	SG64	4-Cm	ce(type VIII)
	WP	Coordinates			Coordinates			Coordinates			Coordinates			Coordinates
			Ge1		(1/4, y, 1/4)	Ge1	8e	(1/4, y, 1/4)	Ge1		(x, 0, 0)	Ge1		(x, 0, 0)
Ge1	1a	(0, 0, 0)	Ge2		(0, y, z)	Ge2	8f	(0, y, z)	Ge2		(0, y, z)	Ge2		(0, y, z)
		(=, =, =)			(~, J, ~)		-	(~, J, ~)		-	(~, J, ~)			(~, J, ~)
			Ge3	8f	(0, y, z)	Ge3	8d	(x, 0, 0)	Ge3	16ø	(x, y, z)	Ge4	8e	(1/4, y, 1/4)
			Ge4		(0, y, z)	Ge4		(x, 0, 0) (x, 0, 0)	Ge4	_	(x, y, z) (x, y, z)	Ge5		(1/4, y, 1/4) $(1/4, y, 1/4)$
Ge2	2d	(1/3, 2/3, 1/2)	Ge5		(x, y, z)	Ge5		(x, y, z)	0.4	105	(x, y, z)	Ge6		(0, y, z)
				108	(x, y, z)		108	$(A, y, \Delta)$				Ge7		(0, y, z) $(0, y, z)$
Fe	3f	(1/2, 0, 0))	Fe1	80	(1/4, y, 1/4)	Fe1	8e	(1/4, y, 1/4)	Fe1	40	(0, 0, 0)	Fe1	4a	(0, 0, 0)
1.6	ÐΙ	(1/2, 0, 0))	Fe2			Fe2	8f		Fe2		(0, 0, 0) (0, 0, 1/2)	Fe2	4a 4b	(0, 0, 0) (0, 0, 1/2)
			Fe3		(0, y, z)	Fe3		(0, y, z)	Fe3					
			Fe4		(x, y, z)	Fe4		(x, y, z)	Fe4		(1/4, 1/4, 0)	Fe4	8c	(1/4, 1/4, 0)
			1.64	TOR	(x, y, z)	1.64	TOR	(x, y, z)	Fe5		(x, y, z)	Fe5		$\begin{array}{c} (\mathrm{x},\mathrm{y},\mathrm{z}) \\ (\mathrm{x},\mathrm{y},\mathrm{z}) \end{array}$
						1			гео	TO5.	(x, y, z)	геэ	105	(X, V, Z)

TABLE X. The corresponding Wyckoff positions and the coordinates of the atoms in the pristine phase and CDW phases with different symmetries. (PART V).

Prist	tine p	phase(P6/mmm)	SG	63-C	mcm(typeI)	SG6	53-Cr	ncm(type II)	SG6	3-Cn	ncm(type III)	SG6	63-Cr	ncm(type IV)
	WP	Coordinates			Coordinates			Coordinates		WP	Coordinates		WP	Coordinates
			Ge1		(0, 0, 0)	Ge1	4a	(0, 0, 0)	Ge1	4c	(0, y, 1/4)	Ge1	4c	(0, y, 1/4)
Ge1	1a	(0, 0, 0)	Ge2		(0, 1/2, 0)	Ge2	4b	(0, 1/2, 0)	Ge2	4c	(0, y, 1/4)	Ge2	4c	(0, y, 1/4)
			Ge3		(1/4, 1/4, 0)	Ge3	8d	(1/4, 1/4, 0)	Ge3	8g	(x, y, 1/4)	Ge3	8g	(x, y, 1/4)
			Ge4	8g	(x, y, 1/4)	Ge4	4c	(0, y, 1/4)	Ge4	8e	(x, 0, 0)	Ge4		(x, 0, 0)
			Ge5	8g	(x, y, 1/4)	Ge5	4c	(0, y, 1/4)	Ge5	8e	(x, 0, 0)	Ge5	8e	(x, 0, 0)
Co2	24	(1/3, 2/3, 1/2)	Ge6	8g	(x, y, 1/4)	Ge6	4c	(0, y, 1/4)	Ge6	16h	(x, y, z)	Ge6	16h	(x, y, z)
Gez	2u	(1/3, 2/3, 1/2)	Ge7	8g	(x, y, 1/4)	Ge7	4c	(0, y, 1/4)						
						Ge8	_	(x, y, 1/4)						
						Ge9	8g	(x, y, 1/4)						
			Fe1	8e	(x, 0, 0)	Fe1	8e	(x, 0, 0)	Fe1	4c	(0, y, 1/4)	Fe1	4c	(0, y, 1/4)
			Fe2	8f	(0, y, z)	Fe2	8f	(0, y, z)	Fe2	4c	(0, y, 1/4)	Fe2	4c	(0, y, 1/4)
			Fe3		(x, y, z)	Fe3		(x, y, z)	Fe3	8g	(x, y, 1/4)	Fe3	8g	(x, y, 1/4)
Fe	3f	(1/2, 0, 0))	Fe4	16h	(x, y, z)	Fe4	16h	(x, y, z)	Fe4	8g	(x, y, 1/4)	Fe4	8g	(x, y, 1/4)
									Fe5	8g	(x, y, 1/4)	Fe5	8g	(x, y, 1/4)
									Fe6	8g	(x, y, 1/4)	Fe6	8g	(x, y, 1/4)
									Fe7	8g	(x, y, 1/4)	Fe7	8g	(x, y, 1/4)
Prist		phase(P6/mmm)	SG6	53-Cr	ncm(type V)	SG6	3-Cn	ncm(type VI)	SG6		cm(type VII)			cm(type VIII)
	WP	Coordinates		WP	Coordinates			Coordinates			Coordinates		WP	Coordinates
				4	(0 1/4)	Ge1	4c	(0 - 1/4)	0 1	8e	(x, 0, 0)			( 0 0)
Ge1			Ge1	4c	(0, y, 1/4)	Ger	40	(0, y, 1/4)	Ge1				8e	(x, 0, 0)
	1a	(0, 0, 0)	Ge2	4c	(0, y, 1/4)	Ge2	4c	(0, y, 1/4)	Ge1 Ge2	8f	(x, 0, 0) (0, y, z)	Ge1 Ge2		(x, 0, 0) (0, y, z)
	1a	(0, 0, 0)	Ge2 Ge3	4c 8g	(0, y, 1/4) (x, y, 1/4)	Ge2 Ge3	4c 8g	(0, y, 1/4) (x, y, 1/4)	Ge2	8f	(0, y, z)	Ge2	8f	(0, y, z)
	1a	(0, 0, 0)	Ge2 Ge3 Ge4	4c 8g 8f	(0, y, 1/4)	Ge2 Ge3 Ge4	4c 8g 8f	(0, y, 1/4)	Ge2 Ge3	8f 8g		Ge2 Ge4	8f 4c	(0, y, z) $(0, y, 1/4)$
	1a	(0, 0, 0)	Ge2 Ge3 Ge4 Ge5	4c 8g 8f 8f	(0, y, 1/4) (x, y, 1/4)	Ge2 Ge3 Ge4 Ge5	4c 8g 8f 8f	(0, y, 1/4) (x, y, 1/4)	Ge2 Ge3 Ge4	8f 8g 8g	(0, y, z)	Ge2 Ge4 Ge5	8f 4c 4c	(0, y, z) (0, y, 1/4) (0, y, 1/4)
Ge?			Ge2 Ge3 Ge4	4c 8g 8f 8f	$ \begin{array}{c} (0, y, 1/4) \\ (x, y, 1/4) \\ \hline (0, y, z) \end{array} $	Ge2 Ge3 Ge4	4c 8g 8f 8f	$ \begin{array}{c} (0, y, 1/4) \\ (x, y, 1/4) \\ \hline (0, y, z) \end{array} $	Ge2 Ge3 Ge4 Ge5	8f 8g 8g 8g	(0, y, z) $(x, y, 1/4)$	Ge2 Ge4 Ge5 Ge6	8f 4c 4c 4c	(0, y, z) (0, y, 1/4) (0, y, 1/4) (0, y, 1/4)
Ge2		(0, 0, 0)	Ge2 Ge3 Ge4 Ge5	4c 8g 8f 8f	$   \begin{array}{c}     (0, y, 1/4) \\     (x, y, 1/4) \\     \hline     (0, y, z) \\     (0, y, z)   \end{array} $	Ge2 Ge3 Ge4 Ge5	4c 8g 8f 8f	$ \begin{array}{c} (0, y, 1/4) \\ (x, y, 1/4) \\ \hline (0, y, z) \\ (0, y, z) \end{array} $	Ge2 Ge3 Ge4 Ge5	8f 8g 8g	$   \begin{array}{c}     (0, y, z) \\     \hline     (x, y, 1/4) \\     (x, y, 1/4)   \end{array} $	Ge4 Ge5 Ge6 Ge7	4c 4c 4c 4c 4c	(0, y, z) (0, y, 1/4) (0, y, 1/4)
Ge2			Ge2 Ge3 Ge4 Ge5	4c 8g 8f 8f	$ \begin{array}{c} (0, y, 1/4) \\ (x, y, 1/4) \\ \hline (0, y, z) \\ (0, y, z) \end{array} $	Ge2 Ge3 Ge4 Ge5	4c 8g 8f 8f	$ \begin{array}{c} (0, y, 1/4) \\ (x, y, 1/4) \\ \hline (0, y, z) \\ (0, y, z) \end{array} $	Ge2 Ge3 Ge4 Ge5	8f 8g 8g 8g	(0, y, z) (x, y, 1/4) (x, y, 1/4) (x, y, 1/4)	Ge2 Ge4 Ge5 Ge6 Ge7 Ge8	8f 4c 4c 4c 4c 8g	(0, y, z) (0, y, 1/4) (0, y, 1/4) (0, y, 1/4) (0, y, 1/4) (x, y, 1/4)
Ge2			Ge2 Ge3 Ge4 Ge5 Ge6	4c 8g 8f 8f 16h	(0, y, 1/4) (x, y, 1/4) (0, y, z) (0, y, z) (x, y, z)	Ge2 Ge3 Ge4 Ge5 Ge6	4c 8g 8f 8f 16h	(0, y, 1/4) (x, y, 1/4) (0, y, z) (0, y, z) (x, y, z)	Ge2 Ge3 Ge4 Ge5 Ge6	8g 8g 8g 8g 8g	(0, y, z) (x, y, 1/4) (x, y, 1/4) (x, y, 1/4) (x, y, 1/4)	Ge4 Ge5 Ge6 Ge7 Ge8 Ge9	4c 4c 4c 4c 4c 8g 8g	(0, y, z) (0, y, 1/4) (0, y, 1/4) (0, y, 1/4) (0, y, 1/4) (x, y, 1/4) (x, y, 1/4)
Ge2			Ge2 Ge3 Ge4 Ge5 Ge6	4c 8g 8f 8f 16h	(0, y, 1/4) (x, y, 1/4) (0, y, z) (0, y, z) (x, y, z) (0, y, 1/4)	Ge2 Ge3 Ge4 Ge5 Ge6	4c 8g 8f 8f 16h	(0, y, 1/4) (x, y, 1/4) (0, y, z) (0, y, z) (x, y, z) (0, y, 1/4)	Ge2 Ge3 Ge4 Ge5 Ge6	8g 8g 8g 8g 8g	(0, y, z) (x, y, 1/4) (x, y, 1/4) (x, y, 1/4) (x, y, 1/4) (x, y, 1/4)	Ge2 Ge4 Ge5 Ge6 Ge7 Ge8 Ge9 Fe1	4c 4c 4c 4c 4c 8g 8g 4a	(0, y, z) $(0, y, 1/4)$ $(0, y, 1/4)$ $(0, y, 1/4)$ $(0, y, 1/4)$ $(x, y, 1/4)$ $(x, y, 1/4)$ $(0, 0, 0)$
Ge2			Ge2 Ge3 Ge4 Ge5 Ge6	4c 8g 8f 8f 16h 4c 4c	(0, y, 1/4) (x, y, 1/4) (0, y, z) (0, y, z) (x, y, z) (x, y, z) (0, y, 1/4) (0, y, 1/4)	Ge2 Ge3 Ge4 Ge5 Ge6	4c 8g 8f 8f 16h 4c 4c	(0, y, 1/4) (x, y, 1/4) (0, y, z) (0, y, z) (x, y, z) (x, y, z) (0, y, 1/4) (0, y, 1/4)	Ge2 Ge3 Ge4 Ge5 Ge6 Fe1 Fe2	8g 8g 8g 8g 8g 4a 4b	(0, y, z) $(x, y, 1/4)$ $(x, y, 1/4)$ $(x, y, 1/4)$ $(x, y, 1/4)$ $(0, 0, 0)$ $(0, 1/2, 0)$	Ge2 Ge4 Ge5 Ge6 Ge7 Ge8 Ge9 Fe1 Fe2	4c 4c 4c 4c 4c 8g 8g 4a 4b	(0, y, z) $(0, y, 1/4)$ $(0, y, 1/4)$ $(0, y, 1/4)$ $(0, y, 1/4)$ $(x, y, 1/4)$ $(x, y, 1/4)$ $(0, 0, 0)$ $(0, 1/2, 0)$
	2d	(1/3, 2/3, 1/2)	Ge2 Ge3 Ge4 Ge5 Ge6 Fe1 Fe2 Fe3	4c 8g 8f 8f 16h 4c 4c 8g	(0, y, 1/4) (x, y, 1/4) (0, y, z) (0, y, z) (x, y, z) (x, y, z) (0, y, 1/4) (0, y, 1/4) (x, y, 1/4)	Ge2 Ge3 Ge4 Ge5 Ge6 Fe1 Fe2 Fe3	4c 8g 8f 8f 16h 4c 4c 8g	(0, y, 1/4) (x, y, 1/4) (0, y, z) (0, y, z) (x, y, z) (x, y, z) (0, y, 1/4) (0, y, 1/4) (x, y, 1/4)	Ge2 Ge3 Ge4 Ge5 Ge6 Fe1 Fe2 Fe3	8g 8g 8g 8g 8g 4a 4b 8d	(0, y, z) (x, y, 1/4) (x, y, 1/4) (x, y, 1/4) (x, y, 1/4) (0, 0, 0) (0, 1/2, 0) (1/4, 1/4, 0)	Ge2 Ge4 Ge5 Ge6 Ge7 Ge8 Ge9 Fe1 Fe2 Fe3	8f 4c 4c 4c 4c 8g 8g 4a 4b 8d	(0, y, z) (0, y, 1/4) (0, y, 1/4) (0, y, 1/4) (0, y, 1/4) (x, y, 1/4) (x, y, 1/4) (0, 0, 0) (0, 1/2, 0) (1/4, 1/4, 0)
Ge2			Ge2 Ge3 Ge4 Ge5 Ge6 Fe1 Fe2 Fe3 Fe4	4c 8g 8f 8f 16h 4c 4c 8g 8g	(0, y, 1/4) (x, y, 1/4) (0, y, z) (0, y, z) (x, y, z) (x, y, z) (0, y, 1/4) (0, y, 1/4) (x, y, 1/4) (x, y, 1/4)	Ge2 Ge3 Ge4 Ge5 Ge6 Fe1 Fe2 Fe3 Fe4	4c 8g 8f 8f 16h 4c 4c 8g 8g	(0, y, 1/4) (x, y, 1/4) (0, y, z) (0, y, z) (x, y, z) (0, y, 1/4) (0, y, 1/4) (x, y, 1/4) (x, y, 1/4)	Ge2 Ge3 Ge4 Ge5 Ge6 Fe1 Fe2 Fe3 Fe4	8g 8g 8g 8g 8g 8d 4a 4b 8d 16h	(0, y, z) (x, y, 1/4) (x, y, 1/4) (x, y, 1/4) (x, y, 1/4) (0, 0, 0) (0, 1/2, 0) (1/4, 1/4, 0) (x, y, z)	Ge2 Ge4 Ge5 Ge6 Ge7 Ge8 Ge9 Fe1 Fe2 Fe3 Fe4	4c 4c 4c 4c 8g 8g 4a 4b 8d 16h	$ \begin{array}{c} (0,y,z) \\ \hline (0,y,1/4) \\ (0,y,1/4) \\ (0,y,1/4) \\ (0,y,1/4) \\ (x,y,1/4) \\ (x,y,1/4) \\ \hline (0,0,0) \\ (0,1/2,0) \\ (1/4,1/4,0) \\ (x,y,z) \\ \end{array} $
	2d	(1/3, 2/3, 1/2)	Ge2 Ge3 Ge4 Ge5 Ge6 Fe1 Fe2 Fe3 Fe4 Fe5	4c 8g 8f 8f 16h 4c 4c 8g 8g 8g	(0, y, 1/4) (x, y, 1/4) (0, y, z) (0, y, z) (x, y, z) (0, y, 1/4) (0, y, 1/4) (x, y, 1/4) (x, y, 1/4) (x, y, 1/4)	Ge2 Ge3 Ge4 Ge5 Ge6 Fe1 Fe2 Fe3 Fe4 Fe5	4c 8g 8f 8f 16h 4c 4c 8g 8g 8g	(0, y, 1/4) (x, y, 1/4) (0, y, z) (0, y, z) (x, y, z) (0, y, 1/4) (0, y, 1/4) (x, y, 1/4) (x, y, 1/4) (x, y, 1/4)	Ge2 Ge3 Ge4 Ge5 Ge6 Fe1 Fe2 Fe3	8g 8g 8g 8g 8g 8d 4a 4b 8d 16h	(0, y, z) (x, y, 1/4) (x, y, 1/4) (x, y, 1/4) (x, y, 1/4) (0, 0, 0) (0, 1/2, 0) (1/4, 1/4, 0)	Ge2 Ge4 Ge5 Ge6 Ge7 Ge8 Ge9 Fe1 Fe2 Fe3	4c 4c 4c 4c 8g 8g 4a 4b 8d 16h	(0, y, z) (0, y, 1/4) (0, y, 1/4) (0, y, 1/4) (0, y, 1/4) (x, y, 1/4) (x, y, 1/4) (0, 0, 0) (0, 1/2, 0) (1/4, 1/4, 0)
	2d	(1/3, 2/3, 1/2)	Ge2 Ge3 Ge4 Ge5 Ge6 Fe1 Fe2 Fe3 Fe4	4c 8g 8f 8f 16h 4c 4c 8g 8g	(0, y, 1/4) (x, y, 1/4) (0, y, z) (0, y, z) (x, y, z) (x, y, z) (0, y, 1/4) (0, y, 1/4) (x, y, 1/4) (x, y, 1/4)	Ge2 Ge3 Ge4 Ge5 Ge6 Fe1 Fe2 Fe3 Fe4	4c 8g 8f 8f 16h 4c 4c 8g 8g	(0, y, 1/4) (x, y, 1/4) (0, y, z) (0, y, z) (x, y, z) (0, y, 1/4) (0, y, 1/4) (x, y, 1/4) (x, y, 1/4)	Ge2 Ge3 Ge4 Ge5 Ge6 Fe1 Fe2 Fe3 Fe4	8g 8g 8g 8g 8g 8d 4a 4b 8d 16h	(0, y, z) (x, y, 1/4) (x, y, 1/4) (x, y, 1/4) (x, y, 1/4) (0, 0, 0) (0, 1/2, 0) (1/4, 1/4, 0) (x, y, z)	Ge2 Ge4 Ge5 Ge6 Ge7 Ge8 Ge9 Fe1 Fe2 Fe3 Fe4	4c 4c 4c 4c 8g 8g 4a 4b 8d 16h	$ \begin{array}{c} (0,y,z) \\ \hline (0,y,1/4) \\ (0,y,1/4) \\ (0,y,1/4) \\ (0,y,1/4) \\ (x,y,1/4) \\ (x,y,1/4) \\ \hline (0,0,0) \\ (0,1/2,0) \\ (1/4,1/4,0) \\ (x,y,z) \\ \end{array} $

- [1] I. Syôzi, "Statistics of kagomé lattice," Progress of Theoretical Physics **6**, 306 (1951).
- [2] A. Mielke, "Ferromagnetic ground states for the Hubbard model on line graphs," Journal of Physics A: Mathematical and General 24, L73 (1991).
- [3] A. Tanaka and H. Ueda, "Stability of ferromagnetism in the Hubbard model on the Kagome lattice," Physical review letters 90, 067204 (2003).
- [4] M. L. Kiesel, C. Platt, and R. Thomale, "Unconventional Fermi surface instabilities in the kagome Hubbard model," Physical review letters 110, 126405 (2013).
- [5] T. Park, M. Ye, and L. Balents, "Electronic instabilities of kagome metals: saddle points and Landau theory," Physical Review B 104, 035142 (2021).
- [6] M. Kang, L. Ye, S. Fang, J.-S. You, A. Levitan, M. Han, J. I. Facio, C. Jozwiak, A. Bostwick, E. Rotenberg, M. K. Chan, R. D. McDonald, D. Graf, K. Kaznatcheev, E. Vescovo, D. C. Bell, E. Kaxiras, J. van den Brink, M. Richter, M. Prasad Ghimire, J. G. Checkelsky, and R. Comin, "Dirac fermions and flat bands in the ideal kagome metal FeSn," Nature materials 19, 163 (2020).
- [7] Y. Xie, L. Chen, T. Chen, Q. Wang, Q. Yin, J. R. Stewart, M. B. Stone, L. L. Daemen, E. Feng, H. Cao, H. Lei, Z. Yin, A. H. MacDonald, and P. Dai, "Spin excitations in metallic kagome lattice FeSn and CoSn," Communications Physics 4, 1 (2021).
- [8] B. C. Sales, J. Yan, W. R. Meier, A. D. Christianson, S. Okamoto, and M. A. McGuire, "Electronic, magnetic, and thermodynamic properties of the kagome layer compound FeSn," Physical Review Materials 3, 114203 (2019).
- [9] S.-H. Do, K. Kaneko, R. Kajimoto, K. Kamazawa, M. B. Stone, J. Y. Y. Lin, S. Itoh, T. Masuda, G. D. Samolyuk, E. Dagotto, W. R. Meier, B. C. Sales, H. Miao, and A. D. Christianson, "Damped Dirac magnon in the metallic kagome antiferromagnet FeSn," Physical Review B 105, L180403 (2022).
- [10] Y.-F. Zhang, X.-S. Ni, T. Datta, M. Wang, D.-X. Yao, and K. Cao, "Ab initio study on spin fluctuations of itinerant kagome magnet FeSn," arXiv preprint arXiv:2209.00187 (2022).
- [11] L. Ye, M. Kang, J. Liu, F. von Cube, C. R. Wicker, T. Suzuki, C. Jozwiak, A. Bostwick, E. Rotenberg, D. C. Bell, L. Fu, R. Comin, and J. G. Checkelsky, "Massive dirac fermions in a ferromagnetic kagome metal," Nature 555, 638 (2018).
- [12] Z. Lin, J.-H. Choi, Q. Zhang, W. Qin, S. Yi, P. Wang, L. Li, Y. Wang, H. Zhang, Z. Sun, L. Wei, S. Zhang, T. Guo, Q. Lu, J.-H. Cho, C. Zeng, and Z. Zhang, "Flatbands and emergent ferromagnetic ordering in fe<sub>3</sub>sn<sub>2</sub> kagome lattices," Physical review letters 121, 096401 (2018).
- [13] N. Morali, R. Batabyal, P. K. Nag, E. Liu, Q. Xu, Y. Sun, B. Yan, C. Felser, N. Avraham, and H. Beidenkopf, "Fermi-arc diversity on surface terminations of the magnetic Weyl semimetal Co<sub>3</sub>Sn<sub>2</sub>S<sub>2</sub>," Science 365, 1286 (2019).
- [14] D. F. Liu, A. J. Liang, E. K. Liu, Q. N. Xu, Y. W. Li, C. Chen, D. Pei, W. J. Shi, S. K. Mo, P. Dudin, T. Kim, C. Cacho, G. Li, Y. Sun, L. X. Yang, Z. K. Liu, S. S. P. Parkin, C. Felser, and Y. L. Chen, "Magnetic

- Weyl semimetal phase in a Kagomé crystal," Science **365**, 1282 (2019).
- [15] K. Kuroda, T. Tomita, M.-T. Suzuki, C. Bareille, A. A. Nugroho, P. Goswami, M. Ochi, M. Ikhlas, M. Nakayama, S. Akebi, R. Noguchi, R. Ishii, N. Inami, K. Ono, H. Kumigashira, A. Varykhalov, T. Muro, T. Koretsune, R. Arita, S. Shin, T. Kondo, and S. Nakatsuji, "Evidence for magnetic Weyl fermions in a correlated metal," Nature materials 16, 1090 (2017).
- [16] J.-X. Yin, S. S. Zhang, G. Chang, Q. Wang, S. S. Tsirkin, Z. Guguchia, B. Lian, H. Zhou, K. Jiang, I. Belopolski, N. Shumiya, D. Multer, M. Litskevich, T. A. Cochran, H. Lin, Z. Wang, T. Neupert, S. Jia, H. Lei, and M. Z. Hasan, "Negative flat band magnetism in a spin-orbit-coupled correlated kagome magnet," Nature Physics 15, 443 (2019).
- [17] J.-X. Yin, W. Ma, T. A. Cochran, X. Xu, S. S. Zhang, H.-J. Tien, N. Shumiya, G. Cheng, K. Jiang, B. Lian, Z. Song, G. Chang, I. Belopolski, D. Multer, M. Litskevich, Z.-J. Cheng, X. P. Yang, B. Swidler, H. Zhou, H. Lin, T. Neupert, Z. Wang, N. Yao, T.-R. Chang, S. Jia, and M. Zahid Hasan, "Quantum-limit Chern topological magnetism in TbMn<sub>6</sub>Sn<sub>6</sub>," Nature 583, 533 (2020).
- [18] M. Li, Q. Wang, G. Wang, Z. Yuan, W. Song, R. Lou, Z. Liu, Y. Huang, Z. Liu, H. Lei, Z. Yin, and S. Wang, "Dirac cone, flat band and saddle point in kagome magnet YMn<sub>6</sub>Sn<sub>6</sub>," Nature communications 12, 1 (2021).
- [19] B. R. Ortiz, L. C. Gomes, J. R. Morey, M. Winiarski, M. Bordelon, J. S. Mangum, I. W. Oswald, J. A. Rodriguez-Rivera, J. R. Neilson, S. D. Wilson, et al., "New kagome prototype materials: discovery of KV3Sb5, RbV3Sb5, and CsV3Sb5," Physical Review Materials 3, 094407 (2019).
- [20] H. Zhao, H. Li, B. R. Ortiz, S. M. Teicher, T. Park, M. Ye, Z. Wang, L. Balents, S. D. Wilson, and I. Zeljkovic, "Cascade of correlated electron states in the kagome superconductor CsV<sub>3</sub>Sb<sub>5</sub>," Nature **599**, 216 (2021).
- [21] H. Chen, H. Yang, B. Hu, Z. Zhao, J. Yuan, Y. Xing, G. Qian, Z. Huang, G. Li, Y. Ye, S. Ma, S. Ni, H. Zhang, Q. Yin, C. Gong, Z. Tu, H. Lei, H. Tan, S. Zhou, C. Shen, X. Dong, B. Yan, Z. Wang, and H.-J. Gao, "Roton pair density wave in a strong-coupling kagome superconductor," Nature 599, 222 (2021).
- [22] B. R. Ortiz, S. M. L. Teicher, Y. Hu, J. L. Zuo, P. M. Sarte, E. C. Schueller, A. M. M. Abeykoon, M. J. Krogstad, S. Rosenkranz, R. Osborn, R. Seshadri, L. Balents, J. He, and S. D. Wilson, "CsV<sub>3</sub>Sb<sub>5</sub>:A z<sub>2</sub> topological kagome metal with a superconducting ground state," Physical Review Letters 125, 247002 (2020).
- [23] Y.-X. Jiang, J.-X. Yin, M. M. Denner, N. Shumiya, B. R. Ortiz, G. Xu, Z. Guguchia, J. He, M. S. Hossain, X. Liu, J. Ruff, L. Kautzsch, S. S. Zhang, G. Chang, I. Belopolski, Q. Zhang, T. A. Cochran, D. Multer, M. Litskevich, Z.-J. Cheng, X. P. Yang, Z. Wang, R. Thomale, T. Neupert, S. D. Wilson, and M. Z. Hasan, "Unconventional chiral charge order in kagome superconductor KV<sub>3</sub>Sb<sub>5</sub>," Nature Materials 20, 1353 (2021).
- [24] C. Mielke, D. Das, J.-X. Yin, H. Liu, R. Gupta, Y.-X. Jiang, M. Medarde, X. Wu, H. C. Lei, J. Chang,

- P. Dai, Q. Si, H. Miao, R. Thomale, T. Neupert, Y. Shi, R. Khasanov, M. Z. Hasan, H. Luetkens, and Z. Guguchia, "Time-reversal symmetry-breaking charge order in a kagome superconductor," Nature **602**, 245 (2022).
- [25] M. M. Denner, R. Thomale, and T. Neupert, "Analysis of Charge Order in the Kagome Metal AV<sub>3</sub>Sb<sub>5</sub>(A= K, Rb, Cs)," Physical Review Letters 127, 217601 (2021).
- [26] Y.-P. Lin and R. M. Nandkishore, "Complex charge density waves at Van Hove singularity on hexagonal lattices: Haldane-model phase diagram and potential realization in the kagome metals AV<sub>3</sub>Sb<sub>5</sub>(A=K, Rb, Cs)," Physical Review B 104, 045122 (2021).
- [27] L. Nie, K. Sun, W. Ma, D. Song, L. Zheng, Z. Liang, P. Wu, F. Yu, J. Li, M. Shan, D. Zhao, S. Li, B. Kang, Z. Wu, Y. Zhou, K. Liu, Z. Xiang, J. Ying, Z. Wang, T. Wu, and X. Chen, "Charge-density-wave-driven electronic nematicity in a kagome superconductor," Nature 604, 59 (2022).
- [28] H. Li, T. T. Zhang, T. Yilmaz, Y. Y. Pai, C. E. Marvinney, A. Said, Q. W. Yin, C. S. Gong, Z. J. Tu, E. Vescovo, C. S. Nelson, R. G. Moore, S. Murakami, H. C. Lei, H. N. Lee, B. J. Lawrie, and H. Miao, "Observation of Unconventional Charge Density Wave without Acoustic Phonon Anomaly in Kagome Superconductors AV<sub>3</sub>Sb<sub>5</sub>(A=Rb, Cs)," Physical Review X 11, 031050 (2021).
- [29] T. Neupert, M. M. Denner, J.-X. Yin, R. Thomale, and M. Z. Hasan, "Charge order and superconductivity in kagome materials," Nature Physics 18, 137 (2022).
- [30] F. Yu, D. Ma, W. Zhuo, S. Liu, X. Wen, B. Lei, J. Ying, and X. Chen, "Unusual competition of superconductivity and charge-density-wave state in a compressed topological kagome metal," Nature communications 12, 1 (2021).
- [31] Y. Xiang, Q. Li, Y. Li, W. Xie, H. Yang, Z. Wang, Y. Yao, and H.-H. Wen, "Twofold symmetry of c-axis resistivity in topological kagome superconductor CsV<sub>3</sub>Sb<sub>5</sub> with inplane rotating magnetic field," Nature communications 12, 1 (2021).
- [32] J. Ge, P. Wang, Y. Xing, Q. Yin, H. Lei, Z. Wang, and J. Wang, "Discovery of charge-4e and charge-6e superconductivity in kagome superconductor csv3sb5," arXiv preprint arXiv:2201.10352 (2022).
- [33] L. Zheng, Z. Wu, Y. Yang, L. Nie, M. Shan, K. Sun, D. Song, F. Yu, J. Li, D. Zhao, S. Li, B. Kang, Y. Zhou, K. Liu, Z. Xiang, J. Ying, Z. Wang, T. Wu, and X. Chen, "Emergent charge order in pressurized kagome superconductor CsV3Sb5," Nature 611, 682 (2022).
- [34] X. Feng, K. Jiang, Z. Wang, and J. Hu, "Chiral flux phase in the Kagome superconductor AV<sub>3</sub>Sb<sub>5</sub>," Science bulletin 66, 1384 (2021).
- [35] K. Jiang, T. Wu, J.-X. Yin, Z. Wang, M. Z. Hasan, S. D. Wilson, X. Chen, and J. Hu, "Kagome superconductors AV3Sb5 (A= K, Rb, Cs)," arXiv preprint arXiv:2109.10809 (2021).
- [36] S.-Y. Yang, Y. Wang, B. R. Ortiz, D. Liu, J. Gayles, E. Derunova, R. Gonzalez-Hernandez, L. Šmejkal, Y. Chen, S. S. Parkin, et al., "Giant, unconventional anomalous hall effect in the metallic frustrated magnet candidate, kv3sb5," Science advances 6, eabb6003 (2020).
- [37] A. Subedi, "Hexagonal-to-base-centered-orthorhombic 4Q charge density wave order in kagome metals KV3Sb5, RbV3Sb5, and CsV3Sb5," Physical Review Materials 6, 015001 (2022).

- [38] J. Zhao, W. Wu, Y. Wang, and S. A. Yang, "Electronic correlations in the normal state of the kagome superconductor KV3Sb5," Physical Review B 103, L241117 (2021).
- [39] H. Tan, Y. Liu, Z. Wang, and B. Yan, "Charge density waves and electronic properties of superconducting kagome metals," Physical review letters 127, 046401 (2021).
- [40] J.-F. Zhang, K. Liu, and Z.-Y. Lu, "First-principles study of the double dome superconductivity in the kagome material CsV3Sb5 under pressure," Physical Review B 104, 195130 (2021).
- [41] J.-G. Si, W.-J. Lu, Y.-P. Sun, P.-F. Liu, and B.-T. Wang, "Charge density wave and pressure-dependent superconductivity in the kagome metal CsV3Sb5: A first-principles study," Physical Review B 105, 024517 (2022).
- [42] Z. Liu, M. Li, Q. Wang, G. Wang, C. Wen, K. Jiang, X. Lu, S. Yan, Y. Huang, D. Shen, J.-X. Yin, Z. Wang, Z. Yin, H. Lei, and S. Wang, "Orbital-selective Dirac fermions and extremely flat bands in frustrated kagomelattice metal CoSn," Nature communications 11, 1 (2020).
- [43] M. Kang, S. Fang, L. Ye, H. C. Po, J. Denlinger, C. Jozwiak, A. Bostwick, E. Rotenberg, E. Kaxiras, J. G. Checkelsky, and R. Comin, "Topological flat bands in frustrated kagome lattice CoSn," Nature communications 11, 1 (2020).
- [44] X. Teng, J. S. Oh, H. Tan, L. Chen, J. Huang, B. Gao, J.-X. Yin, J.-H. Chu, M. Hashimoto, D. Lu, C. Jozwiak, A. Bostwick, E. Rotenberg, G. E. Granroth, B. Yan, R. J. Birgeneau, P. Dai, and M. Yi, "Intertwined magnetism and charge density wave order in kagome FeGe," arXiv preprint arXiv:2210.06653 (2022).
- [45] X. Teng, L. Chen, F. Ye, E. Rosenberg, Z. Liu, J.-X. Yin, Y.-X. Jiang, J. S. Oh, M. Z. Hasan, K. J. Neubauer, B. Gao, Y. Xie, M. Hashimoto, D. Lu, C. Jozwiak, A. Bostwick, E. Rotenberg, R. J. Birgeneau, J.-H. Chu, M. Yi, and P. Dai, "Discovery of charge density wave in a kagome lattice antiferromagnet," Nature 609, 490 (2022).
- [46] J.-X. Yin, Y.-X. Jiang, X. Teng, M. S. Hossain, S. Mardanya, T.-R. Chang, Z. Ye, G. Xu, M. M. Denner, T. Neupert, B. Lienhard, H.-B. Deng, C. Setty, Q. Si, G. Chang, Z. Guguchia, B. Gao, N. Shumiya, Q. Zhang, T. A. Cochran, D. Multer, M. Yi, P. Dai, and M. Z. Hasan, "Discovery of charge order and corresponding edge state in kagome magnet FeGe," Physical Review Letters 129, 166401 (2022).
- [47] C. Setty, C. A. Lane, L. Chen, H. Hu, J.-X. Zhu, and Q. Si, "Electron correlations and charge density wave in the topological kagome metal FeGe," arXiv preprint arXiv:2203.01930 (2022).
- [48] S. Shao, J.-X. Yin, I. Belopolski, J.-Y. You, T. Hou, H. Chen, Y.-X. Jiang, M. S. Hossain, M. Yahyavi, C.-H. Hsu, Y. Feng, A. Bansil, M. Z. Hasan, and G. Chang, "Charge density wave interaction in a Kagome-honeycomb antiferromagnet," arXiv preprint arXiv:2206.12033 (2022).
- [49] H. Miao, T. T. Zhang, H. X. Li, G. Fabbris, A. H. Said, R. Tartaglia, T. Yilmaz, E. Vescovo, S. Murakami, L. X. Feng, K. Jiang, X. L. Wu, A. F. Wang, S. Okamoto, Y. L. Wang, and H. N. Lee, "Charge Dimerization in Strongly Correlated Kagome Magnet FeGe," arXiv preprint arXiv:2210.06359 (2022).

- [50] T. Ohoyama, K. Kanematsu, and K. Yasukōchi, "A new intermetallic compound FeGe," Journal of the Physical Society of Japan 18, 589 (1963).
- [51] O. Beckman, K. Carrander, L. Lundgren, and M. Richardson, "Susceptibility measurements and magnetic ordering of hexagonal FeGe," Physica Scripta 6, 151 (1972).
- [52] L. Häggström, T. Ericsson, R. Wäppling, and E. Karlsson, "Mössbauer study of hexagonal fege," Physica Scripta 11, 55 (1975).
- [53] U. Gäfvert, L. Lundgren, B. Westerstrandh, and O. Beckman, "Crystalline anisotropy energy of uniaxial antiferromagnets evaluated from low field torque data," Journal of Physics and Chemistry of Solids 38, 1333 (1977).
- [54] J. Forsyth, C. Wilkinson, and P. Gardner, "The low-temperature magnetic structure of hexagonal FeGe," Journal of Physics F: Metal Physics 8, 2195 (1978).
- [55] J. Bernhard, B. Lebech, and O. Beckman, "Neutron diffraction studies of the low-temperature magnetic structure of hexagonal FeGe," Journal of Physics F: Metal Physics 14, 2379 (1984).
- [56] J. Bernhard, B. Lebech, and O. Beckman, "Magnetic phase diagram of hexagonal FeGe determined by neutron diffraction," Journal of Physics F: Metal Physics 18, 539 (1988).
- [57] H. Chen, Q. Niu, and A. H. MacDonald, "Anomalous hall effect arising from noncollinear antiferromagnetism," Physical review letters 112, 017205 (2014).
- [58] T. Suzuki, R. Chisnell, A. Devarakonda, Y.-T. Liu, W. Feng, D. Xiao, J. W. Lynn, and J. Checkelsky, "Large anomalous hall effect in a half-heusler antiferromagnet," Nature Physics 12, 1119 (2016).
- [59] S. Nakatsuji, N. Kiyohara, and T. Higo, "Large anomalous hall effect in a non-collinear antiferromagnet at room temperature," Nature 527, 212 (2015).
- [60] F. Kekule, "Studies on aromatic compounds," Annalen der Chemie Und Pharmacial, Leipzig 137, 129 (1865).
- [61] A. I. Liechtenstein, M. Katsnelson, V. Antropov, and V. Gubanov, "Local spin density functional approach to the theory of exchange interactions in ferromagnetic metals and alloys," Journal of Magnetism and Magnetic Materials 67, 65 (1987).
- [62] X. Wan, Q. Yin, and S. Y. Savrasov, "Calculation of magnetic exchange interactions in mott-hubbard systems," Phys. Rev. Lett. 97, 266403 (2006).
- [63] X. Wan, T. A. Maier, and S. Y. Savrasov, "Calculated magnetic exchange interactions in high-temperature superconductors," Phys. Rev. B 79, 155114 (2009).
- [64] A. R. Mackintosh and O. K. Andersen, Electrons at the Fermi surface (1980).
- [65] M. Weinert, R. E. Watson, and J. W. Davenport, "Total-energy differences and eigenvalue sums," Phys. Rev. B 32, 2115 (1985).
- [66] I. Dzyaloshinsky, "A thermodynamic theory of weak fer-

- romagnetism of antiferromagnetics," Journal of Physics and Chemistry of Solids 4, 241 (1958).
- [67] T. Moriya, "Anisotropic superexchange interaction and weak ferromagnetism," Physical Review 120, 91 (1960).
- [68] P. Blaha, K. Schwarz, G. K. H. Madsen, D. Kvasnicka, J. Luitz, et al., "wien2k," An augmented plane wave+ local orbitals program for calculating crystal properties 60 (2001).
- [69] S. H. Vosko, L. Wilk, and M. Nusair, "Accurate spindependent electron liquid correlation energies for local spin density calculations: a critical analysis," Can. J. Phys. 58, 1200 (1980).
- [70] D. D. Koelling and B. N. Harmon, "A technique for relativistic spin-polarised calculations," J. Phys. C 10, 3107 (1977).
- [71] X. Wan, J. Dong, and S. Y. Savrasov, "Mechanism of magnetic exchange interactions in europium monochalcogenides," Physical Review B 83, 205201 (2011).
- [72] X. Wan, V. Ivanov, G. Resta, I. Leonov, and S. Y. Savrasov, "Exchange interactions and sensitivity of the Ni two-hole spin state to Hund's coupling in doped NdNiO<sub>2</sub>," Physical Review B 103, 075123 (2021).
- [73] D. Wang, X. Bo, F. Tang, and X. Wan, "Calculated magnetic exchange interactions in the Dirac magnon material Cu<sub>3</sub>TeO<sub>6</sub>," Phys. Rev. B 99, 035160 (2019).
- [74] N. Metropolis and S. Ulam, "The monte carlo method," J. Am. Stat. Assoc. 44, 335 (1949).
- [75] Z.-X. Shen, C. Su, and L. He, "High-throughput computation and structure prototype analysis for twodimensional ferromagnetic materials," NPJ Comput. Mater. 8, 132 (2022).
- [76] K. Cao, G.-C. Guo, D. Vanderbilt, and L. He, "First-Principles Modeling of Multiferroic RMn<sub>2</sub>O<sub>5</sub>," Phys. Rev. Lett. 103, 257201 (2009).
- [77] P. Baral, N. Ahmed, J. Kumar, S. Nair, and R. Nath, "Synthesis and physical properties of spin-1 honeycomb lattice Pb<sub>6</sub>Ni<sub>9</sub>(TeO<sub>6</sub>)<sub>5</sub>," Journal of Alloys and Compounds 711, 568 (2017).
- [78] R. Chisnell, J. Helton, D. Freedman, D. Singh, R. Bewley, D. Nocera, and Y. Lee, "Topological magnon bands in a kagome lattice ferromagnet," Physical review letters 115, 147201 (2015).
- [79] T. Holstein and H. Primakoff, "Field dependence of the intrinsic domain magnetization of a ferromagnet," Physical Review 58, 1098 (1940).
- [80] D. Wang, J. Yu, F. Tang, Y. Li, and X. Wan, "Determination of the Range of Magnetic Interactions from the Relations between Magnon Eigenvalues at High-Symmetry  $\kappa$  Points," Chinese Physics Letters **38**, 117101 (2021).
- [81] C. J. Bradley and A. P. Cracknell, The Mathematical Theory of Symmetry in Solids: Representation Theory for Point Groups and Space Groups (Oxford University Press, Oxford, 1972).